



**Wire Like Diplatinum, Triplatinum, and Tetraplatinum
Complexes Featuring $X[\text{PtC}\equiv\text{CC}\equiv\text{CC}\equiv\text{CC}\equiv\text{C}]_m\text{PtX}$ Segments;
Iterative Syntheses and Functionalization for Measurements
of Single Molecule Properties**

Journal:	<i>Dalton Transactions</i>
Manuscript ID	DT-ART-02-2019-000870.R1
Article Type:	Paper
Date Submitted by the Author:	29-Mar-2019
Complete List of Authors:	Gladysz, John A.; Texas A&M University, Department of Chemistry Zheng, Qinglin; Institut für Organische Chemie and Interdisciplinary Center for Molecular Materials, Friedrich-Alexander-Universität Erlangen- Nürnberg Schneider, Jakob; Institut für Organische Chemie and Interdisciplinary Center for Molecular Materials, Friedrich-Alexander-Universität Erlangen- Nürnberg Amini, Hashem; Texas A&M University System, Chemistry Hampel, Frank; Institute of Organic Chemistry I, Department of Chemistry and Pharmacy

Wire Like Diplatinum, Triplatinum, and Tetraplatinum Complexes
Featuring $X[\text{PtC}\equiv\text{CC}\equiv\text{CC}\equiv\text{CC}\equiv\text{C}]_m\text{PtX}$ Segments; Iterative Syntheses
and Functionalization for Measurements of Single Molecule
Properties

Qinglin Zheng,^{‡a} Jakob Schneider,^{†a} Hashem Amini,^{●b} Frank Hampel,^a and John A.
Gladysz^{●a,b*}

^aInstitut für Organische Chemie and Interdisciplinary Center for Molecular Materials,
Friedrich-Alexander-Universität Erlangen-Nürnberg, Henkestraße 42, 91054 Erlangen,
Germany

^bDepartment of Chemistry, Texas A&M University, PO Box 30012, College Station,
Texas 77842-3012, USA

E-mail: gladysz@mail.chem.tamu.edu

Abstract

Reaction of $(p\text{-tol}_3\text{P})_2\text{PtCl}_2$ and $\text{Me}_3\text{Sn}(\text{C}\equiv\text{C})_2\text{SiMe}_3$ (1:1/THF/reflux) gives monosubstituted *trans*- $\text{Cl}(p\text{-tol}_3\text{P})_2\text{Pt}(\text{C}\equiv\text{C})_2\text{SiMe}_3$ (63%), which with wet $n\text{-Bu}_4\text{N}^+ \text{F}^-$ yields *trans*- $\text{Cl}(p\text{-tol}_3\text{P})_2\text{Pt}(\text{C}\equiv\text{C})_2\text{H}$ (**2**, 96%). Hay oxidative homocoupling ($\text{O}_2/\text{CuCl}/\text{TMEDA}$) gives all-*trans*- $\text{Cl}(p\text{-tol}_3\text{P})_2\text{Pt}(\text{C}\equiv\text{C})_4\text{Pt}(Pp\text{-tol}_3)_2\text{Cl}$ (**3**, 68%). Reaction of **3** and $\text{Me}_3\text{Sn}(\text{C}\equiv\text{C})_2\text{SiMe}_3$ (1:1/rt) affords monosubstituted all-*trans*- $\text{Cl}(p\text{-tol}_3\text{P})_2\text{Pt}(\text{C}\equiv\text{C})_4\text{Pt}(Pp\text{-tol}_3)_2(\text{C}\equiv\text{C})_2\text{SiMe}_3$ (46%), which is converted by a similar desilylation/homocoupling sequence to all-*trans*- $\text{Cl}[(p\text{-tol}_3\text{P})_2\text{Pt}(\text{C}\equiv\text{C})_4]_3\text{Pt}(Pp\text{-tol}_3)_2\text{Cl}$ (**7**; 79%). Reaction of $(p\text{-tol}_3\text{P})_2\text{PtCl}_2$ and excess $\text{H}(\text{C}\equiv\text{C})_2\text{SiMe}_3$ ($\text{HNEt}_2/\text{cat. CuI}$) gives *trans*- $\text{Me}_3\text{Si}(\text{C}\equiv\text{C})_2\text{Pt}(Pp\text{-tol}_3)_2(\text{C}\equiv\text{C})_2\text{SiMe}_3$ (78%), which with wet $n\text{-Bu}_4\text{N}^+ \text{F}^-$ affords *trans*- $\text{H}(\text{C}\equiv\text{C})_2\text{Pt}(Pp\text{-tol}_3)_2(\text{C}\equiv\text{C})_2\text{H}$ (96%). Hay oxidative cross coupling with **2** (1:4) gives all-*trans*- $\text{Cl}[(p\text{-tol}_3\text{P})_2\text{Pt}(\text{C}\equiv\text{C})_4]_2\text{Pt}(Pp\text{-tol}_3)_2\text{Cl}$ (**10**, 36%) along with homocoupling product **3** (33%). Reaction of **3** and $\text{Me}_3\text{Sn}(\text{C}\equiv\text{C})_2\text{SiMe}_3$ (1:2/rt) yields all-*trans*- $\text{Me}_3\text{Si}(\text{C}\equiv\text{C})_2(p\text{-tol}_3\text{P})_2\text{Pt}(\text{C}\equiv\text{C})_4\text{Pt}(Pp\text{-tol}_3)_2(\text{C}\equiv\text{C})_2\text{SiMe}_3$ (**17**, 77%), which with wet $n\text{-Bu}_4\text{N}^+ \text{F}^-$ gives all-*trans*- $\text{H}(\text{C}\equiv\text{C})_2(p\text{-tol}_3\text{P})_2\text{Pt}(\text{C}\equiv\text{C})_4\text{Pt}(Pp\text{-tol}_3)_2(\text{C}\equiv\text{C})_2\text{H}$ (96%). Reaction of **3** and excess Me_3P gives all-*trans*- $\text{Cl}(\text{Me}_3\text{P})_2\text{Pt}(\text{C}\equiv\text{C})_4\text{Pt}(\text{PMe}_3)_2\text{Cl}$ (**4**, 86%). A model reaction of *trans*- $(p\text{-tol})(p\text{-tol}_3\text{P})_2\text{PtCl}$ and KSAc yields *trans*- $(p\text{-tol})(p\text{-tol}_3\text{P})_2\text{PtSAc}$ (**12**, 75%). Similar reactions of **3**, **7**, **10**, and **4** give all-*trans*- $\text{AcS}[(\text{R}_3\text{P})_2\text{Pt}(\text{C}\equiv\text{C})_4]_n\text{Pt}(\text{PR}_3)_2\text{SAc}$ (76-91%). The crystal structures of **3**, **17**, and **12** are determined. The first exhibits a chlorine-chlorine distance of 17.42 Å; those in **10** and **7** are estimated as 30.3 Å and 43.1 Å.

[†]Electronic supplementary information (ESI) available: Cyclic voltammogram traces. CCDC 1899327 (**3**), 1898997 (**17**), and 1898998 (**12**). For ESI and crystallographic data in CIF or other electronic format see DOI: 10.1039/c5sc03xxxx

[‡]Present address: THOR Specialty Chemical Company Limited, 182 Jingang Ave., New District, Zhenjiang, Jiangsu, 212132 PRC.

†Present address: Delmar Chemicals Inc., 9321 Rue Airlie, Montréal, QWC, H8R 2B2, Canada

Key words: platinum, polyynes, phosphine, thioacetate, crystal structures, homocoupling
submitted to *Dalton Transactions*

Introduction

There has been great interest in compounds in which sp carbon chains span two transition metals.¹ In particular, polyynediyl moieties, $-(C\equiv C)_n-$, can be viewed as the ultimate in unsaturated bridging organic ligands, as they can never be twisted out of conjugation. As the field has developed, increased attention has been given to compounds with more complex arrays of sp carbon chains. Some of these are of interest with respect to molecular devices and materials properties,² while others possess a structural aesthetic and attract those drawn to synthetic challenges.³ Some of the earliest practitioners in this field trained their sights on one dimensional polymers of the types **Ia**⁴ and **Ib**^{4d,5} (Figure 1), and second generation efforts⁶ included a few homologs with $(C\equiv C)_3$ segments.^{6a} More extensive attention has been given to arylene expanded analogs such as **II**,^{4a,6,7} which we note for the record but view any further digression as beyond the scope of this study.

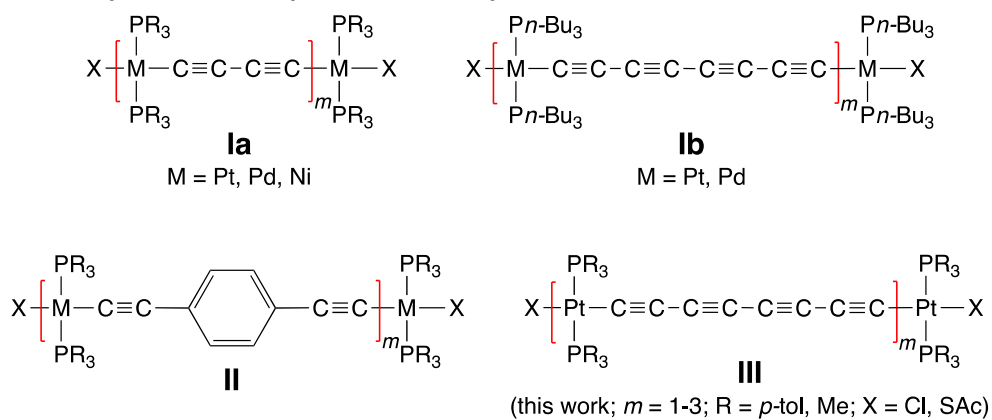


Figure 1. Previously synthesized polymers (I, II) and title complexes (III).

Efforts in our laboratory have focused on the elaboration of $Re(C\equiv C)_nRe$ ⁸ and $Pt(C\equiv C)_nPt$ ⁹ systems. These building blocks are available with chain lengths of up to twenty eight sp carbon atoms, although as a side remark the current "record" is held by purely organic compounds with bulky substituted trityl endgroups.¹⁰ We were attracted to a related challenge, namely the synthesis of longitudinal arrays based upon $-L_2PtC\equiv CC\equiv CC\equiv CC\equiv C-$ repeat units. Despite the work on systems of the type I,^{4,6} and

the collateral isolation of two trimetallic complexes with $-L_2MC\equiv CC\equiv C-$ repeat units (discussion section),^{4b} to our knowledge iterative synthetic strategies that afford families of $-[L_yM(C\equiv C)_n]_m-$ species remain unknown. When such series are available, the gradual transition of physical and chemical properties to the macromolecular limit can be mapped.

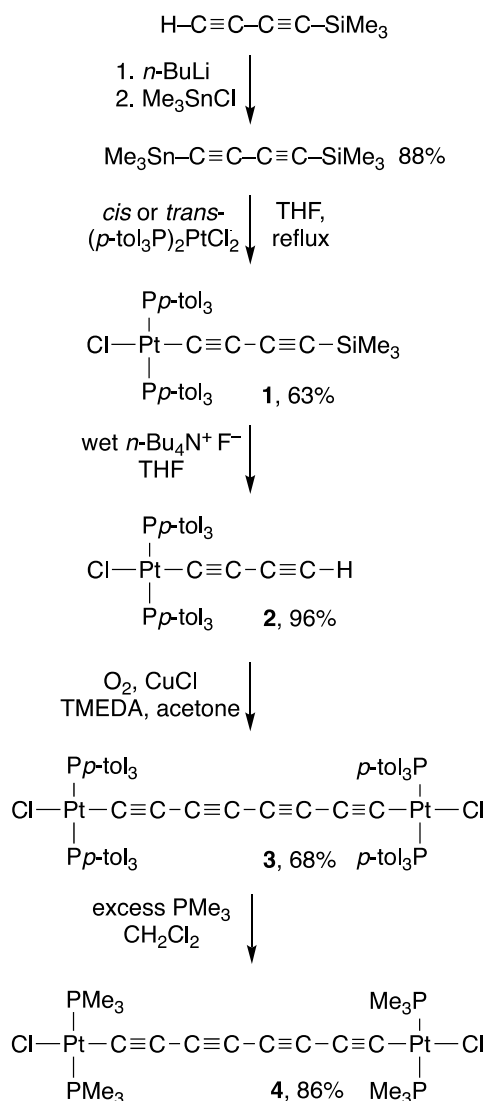
In this paper, we report efficient syntheses of such assemblies bearing two, three, and four platinum atoms, each terminating in platinum-chloride bonds. We then introduce thioacetate ligands at the termini, which can be transformed to the equivalent of "alligator clips" for single molecule conductivity and other measurements.¹¹ The first series of reactions have been communicated,¹² but the second have never been disclosed, despite a published investigation of the charge transport properties of one of the sulfur containing complexes.¹³ Representative crystal structures are also described, together with in depth analyses of spectroscopic and thermal properties. A detailed investigation of the photophysical properties of the dichloride complexes has been reported separately.¹⁴

Results

1. Syntheses of Diplatinum Complexes. For syntheses of diplatinum polyynediyl complexes $L_yPt(C\equiv C)_nPtL_y$ (IV),⁹ monofunctional monoplatinum building blocks such as *trans*-Ar'(Ar₃P)₂PtCl suffice. Under appropriate conditions, the chloride ligands can be replaced by a variety of alkynyl groups. The oxidative homocoupling of $L_yPt(C\equiv C)_{n/2}H$ species then affords the target molecules IV, although the precursors are often generated *in situ* due to rapidly decreasing stabilities when $n > 2$. In contrast, the iterative synthesis of longitudinally extended homologs III requires difunctional platinum building blocks, such as the dichloride complex *trans*-(Ar₃P)₂PtCl₂. However, at certain stages monofunctionalizations are likely to be necessary. Thus, reactions with terminal alkynes and diynes (1:1 mol ratios) were screened under conditions previously employed for related monochloride complexes. Unfortunately, mixtures of bis(alkynyl),

the desired monoalkynyl/monochloride, and unreacted dichloride complexes were always obtained.

Accordingly, the previously reported unsymmetrical stannyl/silyl diyne $\text{Me}_3\text{Sn}(\text{C}\equiv\text{C})_2\text{SiMe}_3$ was prepared by the sequential reaction of $\text{H}(\text{C}\equiv\text{C})_2\text{SiMe}_3$ with *n*-BuLi and Me_3SnCl , as shown in Scheme 1.¹⁵ It was then combined (1:1 mol ratio) with either *cis*- or *trans*-(*p*-tol₃P)₂PtCl₂ in refluxing THF.¹⁶ Me_3SnCl elimination occurred in preference to Me_3SiCl elimination to give the monosubstituted product *trans*-Cl(*p*-tol₃P)₂Pt(C≡C)₂SiMe₃ (1) in 63% yield after workup.¹⁷ Indeed, reactions of other platinum dichloride complexes L_2PtCl_2 and the trimethylstannyl alkyne $\text{Me}_3\text{SnC}\equiv\text{CPh}$ give the monosubstitution products *trans*-ClL₂PtC≡CPh in good yields.¹⁸



Scheme 1. Syntheses of diplatinum complexes.

Complex 1 and all other new compounds below were characterized by microanalysis, NMR (^1H , $^{13}\text{C}\{^1\text{H}\}$, $^{31}\text{P}\{^1\text{H}\}$) and IR spectroscopy, and mass spectrometry. The IR $\nu_{\text{C}\equiv\text{C}}$ values and ^{31}P NMR data are provided in Table 1, and ^{13}C NMR data are listed in Table 2. In all cases, *trans* stereochemistry could be assigned based upon the diagnostic magnitudes of the $^1J_{\text{PPt}}$ values (2518-2615 Hz).¹⁹ Other data are analyzed in the discussion section.

Complex 1 was elaborated to a diplatinum octatetraynediyl complex similarly to related trialkylsilylbutadiynyl adducts described earlier.^{9a,b} First, reaction with wet *n*-Bu₄N⁺ F⁻ gave the butadiynyl complex *trans*-Cl(*p*-tol₃P)₂Pt(C≡C)₂H (2) in 96% yield.

Subsequent oxidative homocoupling under Hay conditions (O_2 , CuCl, TMEDA, acetone)²⁰ afforded the target complex **3** (Scheme 1) as a yellow solid in 68% yield. The thermal stabilities of **3** and all other octatetraynediyl complexes were characterized by various measures as given in Table 3. Their UV-visible spectra were also recorded, as summarized in Table 4 and depicted in Figure 2.

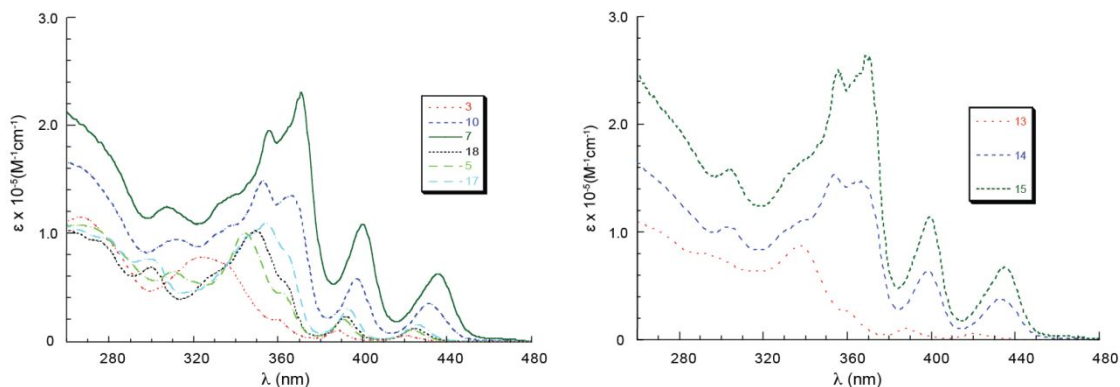
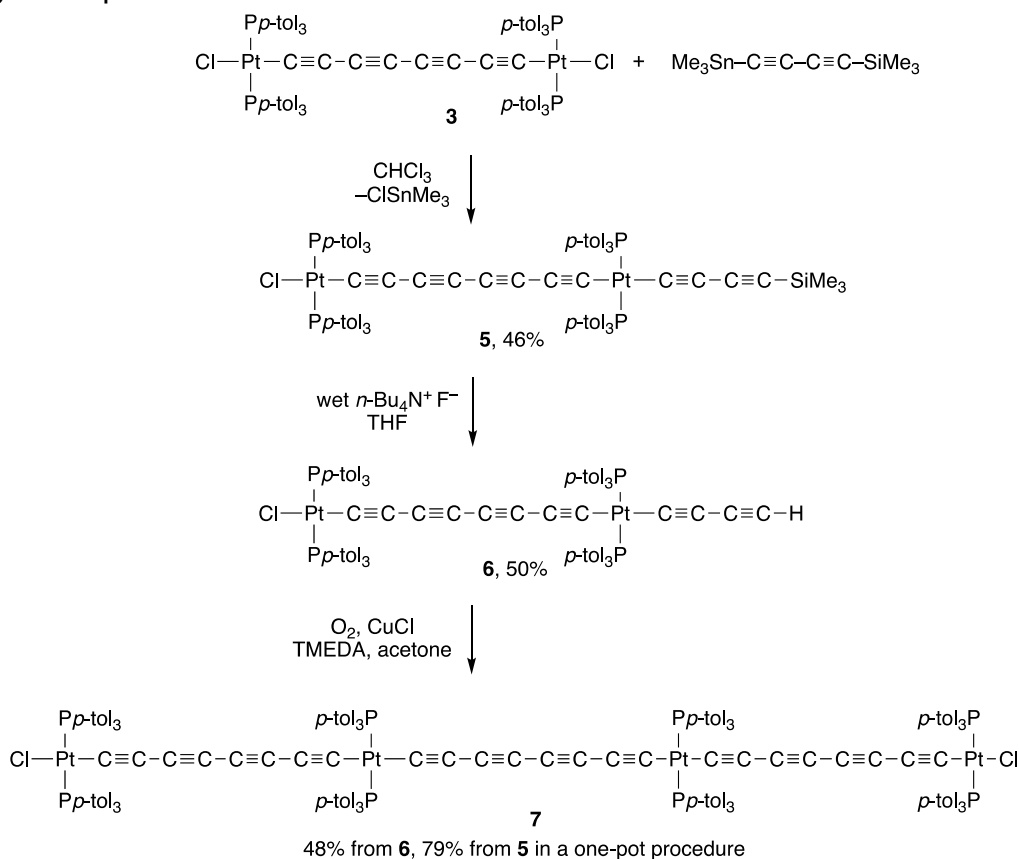


Figure 2. UV-visible spectra (for concentrations and ϵ values, see Table 4).

The application of this family of compounds as "molecular wires" requires introducing functionality that can effectively bind gold or another suitable surface or break junction tip.¹¹ Towards this end, moderately bulky *cis* triarylphosphine ligands such as *p*-tol₃P may weaken the attachment. Thus, the feasibility of a "post synthetic modification" for introducing smaller phosphines was tested. As shown in Scheme 1, **3** and Me₃P (4.8 equiv) were combined in CH₂Cl₂. After 1 h, workup gave the tetrakis(trimethylphosphine) complex **4** (Scheme 1) in 86% yield.

2. Syntheses of Tri- and Tetraplatinum Complexes. It was next sought to elaborate **3** to higher homologs by selectively introducing a single butadiynyl ligand. As shown in Scheme 2, reaction with Me₃Sn(C≡C)₂SiMe₃ (1.0 equiv) gave the monosubstituted trimethylsilylbutadiynyl complex **5** (Scheme 2) in 46% yield after chromatography. Presumably some disubstituted product also formed, but was removed on the column. Next, a desilylation/homocoupling sequence analogous to that used to convert **2** to **3** was carried out. This gave first the butadiynyl complex **6** (50%; Scheme

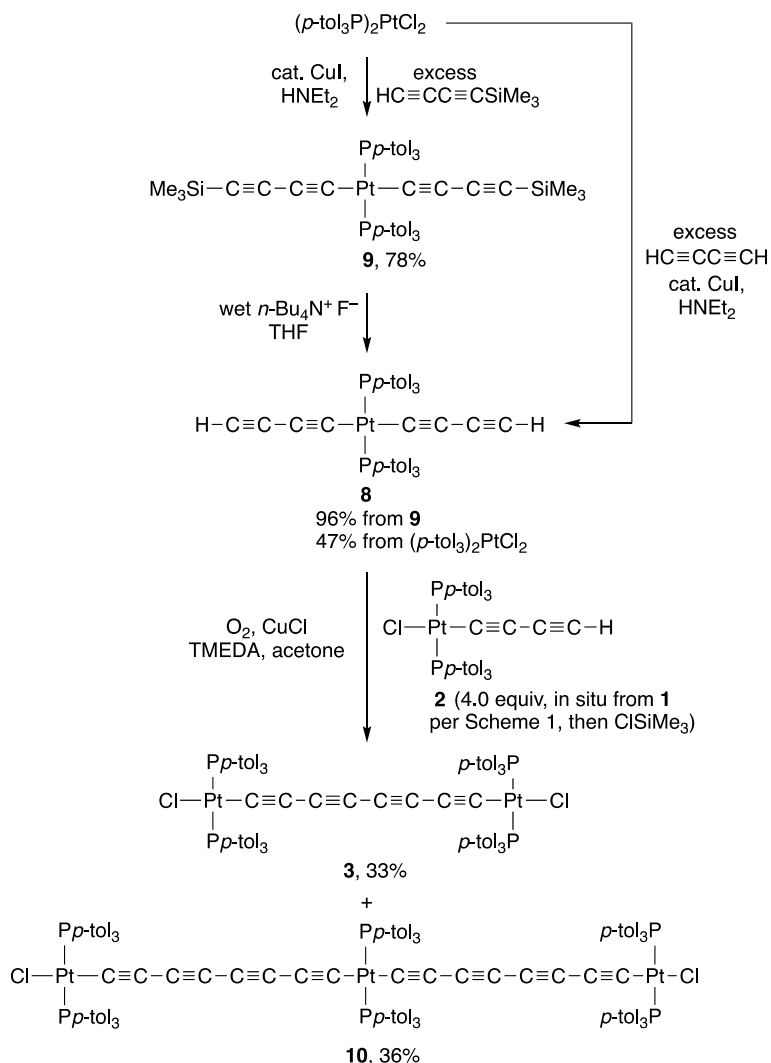
2) and then the tetraplatinum target (**7**; 48% or 24% from **5**) as an orange solid. Curiously, the desilylation of **5** was much slower than that of **1**. When the conversion of **5** to **7** was carried out in a single pot without purification of the intermediate **6**, the overall yield improved to 79%.



Scheme 2. Synthesis of tetraplatinum complex **7**.

To access the corresponding triplatinum species, a two-fold cross coupling was envisioned as shown in Scheme 3. In a standard procedure for the formation of platinum-alkynyl linkages,²¹ either *cis*- or *trans*-(*p*-tol₃P)₂PtCl₂ was condensed with excess H(C≡C)₂H in HNEt₂ in the presence of CuI.^{16,17} In both cases, workups gave the bis(butadiynyl) complex *trans*-H(C≡C)₂Pt(P*p*-tol₃)₂(C≡C)₂H (**8**, 47%).²² However, a two step procedure gave somewhat better overall yields. First, (*p*-tol₃P)₂PtCl₂ and H(C≡C)₂SiMe₃ were similarly condensed to give *trans*-Me₃Si(C≡C)₂Pt(P*p*-tol₃)₂(C≡C)₂SiMe₃ (**9**; 78%).²² Both trimethylsilyl groups could then be removed with wet *n*-Bu₄N⁺ F⁻ to give **8** (96%). Next, in a one-pot sequence, **1** was similarly de-

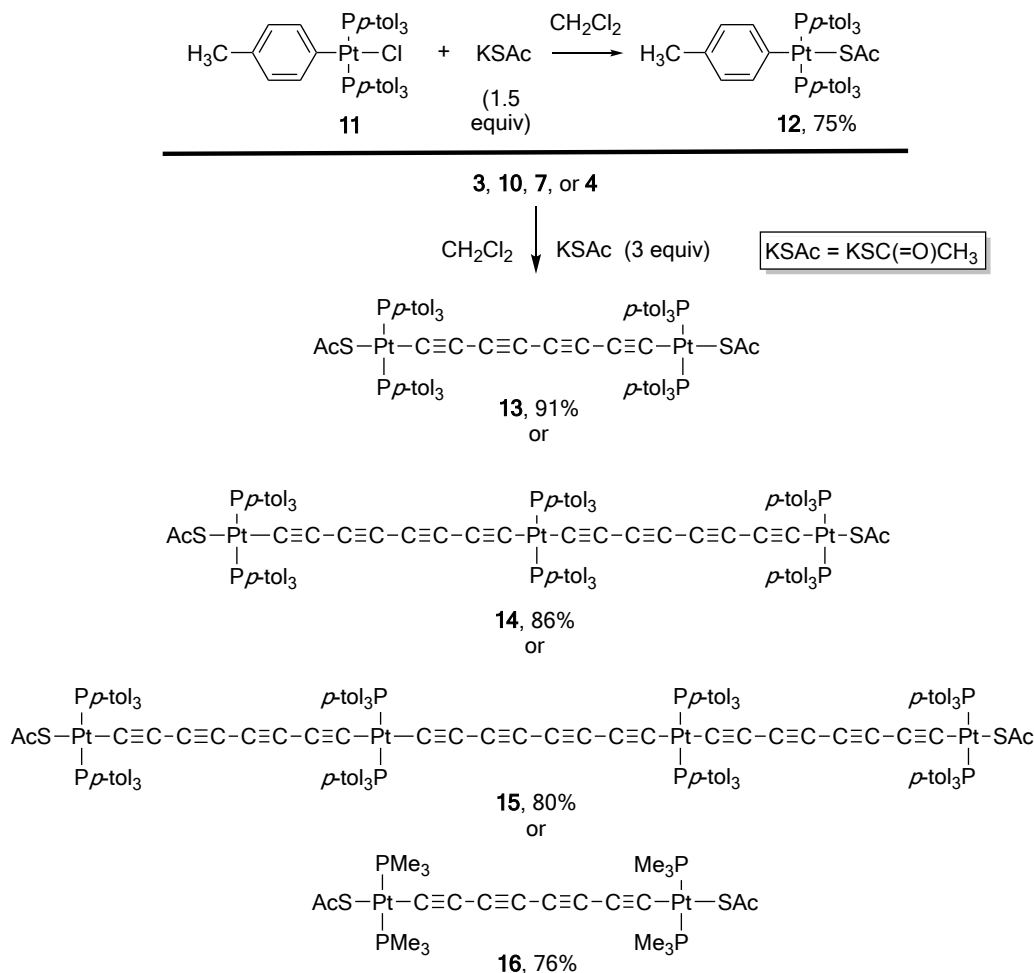
silylated to **2**, and Me_3SiCl was added to scavenge fluoride ion.^{9a} Then **8** was added (0.25 equiv or 1:4 mol ratio) and cross coupling effected under Hay conditions. Chromatography gave the triplatinum target **10** (36% based upon **8**; Scheme 3). Some homocoupling product **3** also formed (33% based upon **1**), but could be separated.



Scheme 3. Synthesis of the triplatinum complex **10**.

3. Thioacetate complexes. Covalent connections to gold electrodes, as well as the formation of self assembled monolayers on gold surfaces, are most commonly effected using -SH groups.¹¹ Since thiols can be prone to oxidation, they are often generated *in situ* by basic hydrolyses or NaBH_4 reductions of the corresponding thioacetates.^{11,23,24} Palladium halide complexes are known to readily react with

potassium thioacetate (KSAc) to give thioacetate complexes.²⁵ Thus, a model reaction was carried out with the platinum chloride complex *trans*-(*p*-tol)(*p*-tol₃P)₂PtCl (**11**)^{9b} as shown in Scheme 4 (top). Workup gave the expected substitution product *trans*-(*p*-tol)(*p*-tol₃P)₂Pt(SAc) (**12**) in 75% yield.

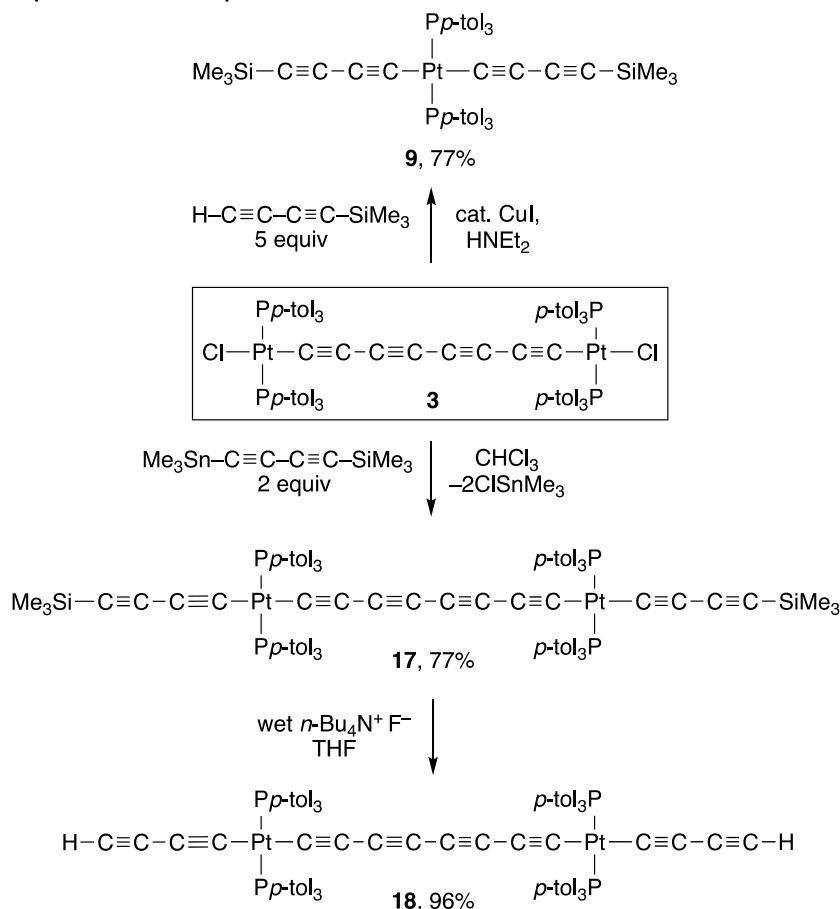


Scheme 4. Syntheses of thioacetate complexes.

Similar conditions were then applied to the di-, tri-, and tetraplatinum complexes **3**, **10**, and **7**, as well as trimethylphosphine-substituted **4**. As shown in Scheme 4 (bottom), the corresponding bis(thioacetate) complexes **13-16** were isolated in 76-91% yields. The IR $\nu_{\text{C}=\text{O}}$ bands were observed at 1613-1625 cm^{-1} (m; Table 1), with those for the homologous series **13-15** monotonically increasing with the number of repeat units m . The IR $\nu_{\text{C}-\text{S}}$ bands were found at 942-946 cm^{-1} (m).

4. Other chemistry. In the course of developing the syntheses in Schemes 1-3 or

exploring routes to still higher homologs, a number of other reactions were evaluated. One dead end that merits emphasis is shown in Scheme 5. The reaction of the diplatinum complex **3** and excess $\text{H}(\text{C}\equiv\text{C})_2\text{SiMe}_3$ was carried out under standard conditions (cat. CuI/HNEt_2) with the idea of replacing both chloride ligands with trimethylsilylbutadiynyl groups. However, workup gave the monoplatinum complex **9**, a key building block in Scheme 3, in 77% yield. This indicates that platinum-polyynediyl linkages can, under appropriate conditions, undergo net σ bond metatheses with terminal alkynes, and suggests a general way to deoligomerize any of the species **III** back to monoplatinum complexes.



Scheme 5. Additional platinum-carbon bond forming reactions.

With regard to possible extension of the title series, **3** was treated with 2 equiv of $\text{Me}_3\text{Sn}(\text{C}\equiv\text{C})_2\text{SiMe}_3$ under conditions similar to those used for the 1:1 reaction in Scheme 3. As shown in Scheme 5, the expected disubstitution product **17** could be

isolated in 77% yield. Numerous efforts were made to selectively protodesilylate *one* of the termini. However, satisfactory conditions were never found. Nonetheless, both trimethylsilyl groups could be efficiently removed with wet $n\text{-Bu}_4\text{N}^+ \text{F}^-$, affording **18** (Scheme 5) in 96% yield. The monosilylated intermediate would be an attractive precursor to another tetraplatinum complex, and **18** is a potential monomer for oxidative polymerizations that would yield higher homologs of the title complexes.

5. Other characterization. The diplatinum complexes **3** and **17** could both be crystallized (the former as a diacetone solvate). The crystal structures were determined as outlined in Table 5 and the experimental section. The molecular structures are depicted in Figure 3, and key interatomic distances and bond angles are provided in Table 6. In both cases, the sp carbon chains adopted S-shaped conformations containing an inversion center. These features have also been seen in the structures of other tetraynes and higher polyynes.^{1b} All bond lengths and angles were within the ranges found in related diplatinum complexes.^{1b} The platinum-platinum distances were 12.750-12.833 Å, and the chlorine-chlorine distance in **3** was 17.422 Å. Although single crystals of **10** and **7** could not be obtained, the chlorine-chlorine distances can be estimated as 30.3 and 43.1 Å, respectively, using the platinum-platinum and platinum-chlorine distances in **3**.

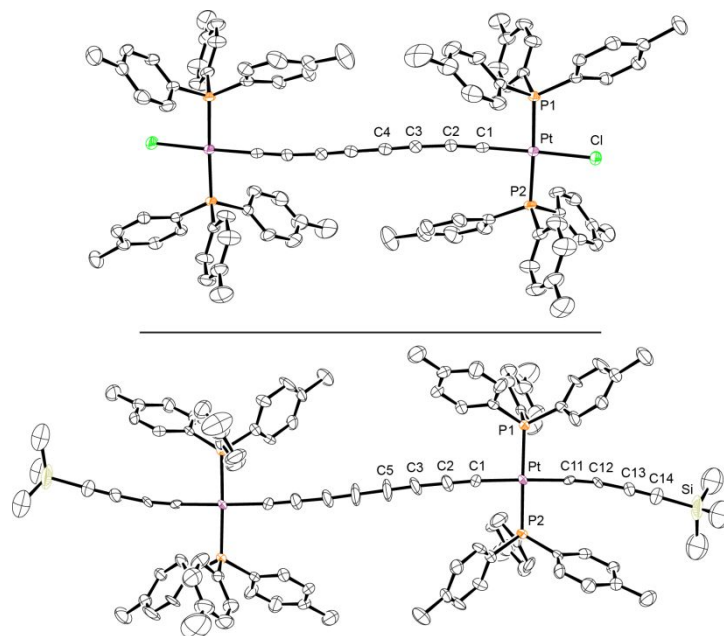


Figure 3. Thermal ellipsoid plots (50% probability) of **3**·(acetone)₂ with the acetone molecules omitted (top) and **17** (bottom).

Single crystals of the model thioacetate complex **12** could also be obtained, and the structure was similarly determined. The results are given in Figure 4, and confirm that none of the several alternative thioacetate coordination modes²⁵ are operative. The bond distances and angles about platinum and the thioacetate carbon atom are unexceptional. All are in good agreement with those in two other platinum(II) thioacetate complexes, both of which are dianionic (most pronounced difference: Pt-S 2.3793(7) Å in **12** vs. 2.3048(4)-2.3312(4) Å in others).²⁶ Unfortunately, none of the other thioacetate complexes in Scheme 4 could be crystallized.

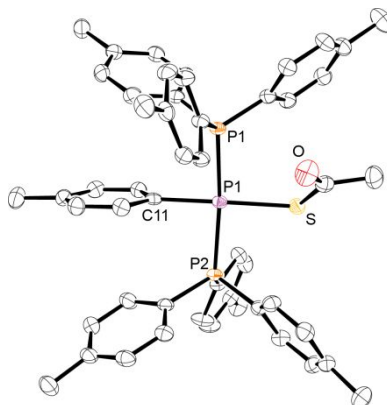


Figure 4. Thermal ellipsoid plot (50% probability) of **12**. Key bond distances (Å) and angles (°): Pt-C₁₁, 2.046(3); Pt-S, 2.3793(7); Pt-P₁, 2.3117(6); Pt-P₂, 2.3020(6); S-C, 1.745(3); C=O, 1.213(4); C₁₁-Pt-S, 170.50(7); P₁-Pt-P₂, 172.92(2); Pt-S-C, 110.89(10); S-C-O, 125.2(2); O-C-C, 121.2(3).

Cyclic voltammograms of **3**, **10**, and **7** showed partially reversible one-electron oxidations, as summarized in Table 7 and depicted in Figure s1 in the electronic supplementary information (ESI). The $i_{c/a}$ values decreased with the Pt/C_{sp} chain length, as seen for several series of diplatinum polyynediyl complexes.^{9a,b} In contrast, the corresponding thioacetate complexes did not show any appreciable anodic current following the initial oxidation.

Discussion

1. Related complexes and synthetic methodology. As briefly noted in the introduction, two trimetallic group 10 complexes with two butadiynediyl linkages have been previously reported,^{4b} and their syntheses are shown in Scheme 6 (**20**, top).²⁷ An analogous route to our triplatinum complex **10** would be challenging due to the very poor stabilities of octatetraynyl ($L_nM(C\equiv C)_4H$) complexes, even at low temperatures.^{9a,b} Using other types of metal-carbon bond forming reactions, we have isolated an adduct with a *trans*-Re(C≡C)₂Pd(C≡C)₂Re linkage,²⁸ and some Au(C≡C)_{*n*}Ru(C≡C)_{*n*}Au species (*n* = 2-4) have been recently reported.^{2b} Berke has synthesized tetrairon complexes with Fe(C≡C)₂Fe(C≡C)₂Fe(C≡C)₂Fe backbones, as well as diron analogs, and demonstrated that stable junctions to gold STM tips can be generated from Me₃Sn-(C≡C)₂Fe moieties.³⁰

Pt(C≡C)₂H species that could undergo oxidative homocoupling to an octaplatinum complex. Another approach would involve converting both termini of triplatinum complex **10** to Pt(C≡C)₂H moieties.²⁹ A subsequent oxidative cross coupling with excess **2** – analogous to the reaction of **8** and excess **2** used to access **10** – would afford a pentaplatinum complex.

We are also interested in altering the dimensionality in which the polyynediyl segments in the title complexes are arrayed. In a complementary investigation, we have described efficient routes to adducts in which two Pt(C≡C)_{*n*}Pt moieties (*n* = 3, 4) bear lateral (as opposed to longitudinal) relationships, as illustrated by **21** in Scheme 6 (middle).^{9g} These may be regarded as precursors to multistranded molecular wires. A priori, there is no impediment to extending the synthetic methodology (treatment of triarylphosphine precursors with the 1,3-diphosphine Ph₂P(CH₂)₃PPh₂) to **3**, **10**, and **7**.

Another approach to altering the dimensionality of the title complexes would involve reactions with 1,2-diphosphines. For example, we find that triarylphosphine ligands in diplatinum polyynediyl complexes *trans,trans*-Ar'(Ar₃P)₂Pt(C≡C)₄Pt(PAr₃)₂Ar' can be replaced by Ph₂PCH₂CH₂PPh₂^{9g} and presumably tetraalkyl analogs Me₂PCH₂CH₂PMe₂. This results in a *cis,cis* isomer.³¹ As shown in the hypothetical reaction in Scheme 6 (bottom), analogous substitutions would delinearize or "kink" the -L₂PtC≡CC≡CC≡CC≡C- repeat units, transforming them to two (or three) dimensional structures that have tantalizing possibilities as precursors to molecular polygons and related species.

2. Analyses of properties. As summarized in Table 3, the thermal stabilities of the title dichloride and bis(thioacetate) complexes are striking. They all persist to ≥160 °C in the solid state. In most cases, exotherms are detected, but for **3**, **10**, and **7**, mass loss begins only at much higher temperatures. Solutions of **3**, **10**, **7**, and the thioacetate analogs showed no deterioration after several hours in air. These data auger well for the isolation of higher homologs.

As shown in Table 1, the ^{31}P NMR signals of the phosphine ligands on the internal platinum atoms ($\equiv\text{CPt}(\text{P}\rho\text{-tol}_3)_2\text{C}\equiv$) are 2.7-3.4 ppm upfield of those on the terminal platinum atoms (δ 16.7-16.8 vs. 19.4-20.1 ppm). In contrast, the ^{13}C NMR signals of the sp carbon atoms on the internal platinum atoms ($\equiv\text{CPtC}\equiv$) are downfield (105.8-106.1 ppm for **10**, **7**, and the SAc analogs) from those on the terminal platinum atoms ($\text{XPtC}\equiv$; X = Cl, 83.7 ppm; X = SAc, 95.3 ppm). The same trend is found for the corresponding $\text{PtC}\equiv\text{C}$ carbon atoms (X = Cl, 95.9 vs. 88.5-88.6 ppm; X = SAc, 95.9 vs. 92.9-93.0 ppm). As noted for many other octatetraynediyl complexes, the chemical shifts of the four innermost sp carbon atoms fall into a relatively narrow range (58.7-63.6 ppm).^{8,9} NICS calculations that may aid additional assignments have recently been reported.³²

As summarized in Table 1, the IR $\nu_{\text{C}\equiv\text{C}}$ patterns are practically identical for the title dichloride and bis(thioacetate) complexes, regardless of number of $-\text{L}_2\text{PtC}\equiv\text{CC}\equiv\text{CC}\equiv\text{CC}\equiv\text{C}-$ repeat units (2138-2142 cm^{-1} m, 1999-2008 cm^{-1} w vs. 2142-2150 cm^{-1} m, 1999-2011 cm^{-1} w). In contrast, the UV-visible spectra (Figure 2 and Table 4) show progressively more intense and red-shifted absorptions with increased chain length. Accordingly, the tetraplatinum complexes (**7**, **15**) are orange, but the others are yellow. The homology between the spectra of **7** and **15**, as well as the triplatinum complexes **10** and **14** (Figure 2), is striking. These trends indicate substantial electronic interactions between the tetrayne moieties, which in a separate study has been principally ascribed to $d\pi(\text{Pt})-p\pi(\text{C})$ overlap.¹⁴ This overlap furthermore plays a role in the excited state photophysics of **10** and **7**.¹⁴ It is also apparent that longer wavelength absorptions intensify and red-shift when chloride ligands are replaced by $(\text{C}\equiv\text{C})_2\text{SiMe}_3$ or $(\text{C}\equiv\text{C})_2\text{H}$ ligands (Figure 2).

As noted in the results section, there are no exceptional bond lengths or angles in the crystal structures in Figures 3 and 4. However, the structures do convey a visual impression that anchoring a $-\text{S}-\text{Pt}$ linkage to a gold break junction, STM tip, or the like

has the potential to be sterically impeded by *cis*-P*ρ*-tol₃ ligands. The Au-S distances on gold surfaces have been calculated to be 2.36 Å,³³ which translates to Au...Pt distances of about 4.7 Å for any -S-Pt species derived from our complexes. Although crystal structures could not be obtained for the analogous trimethylphosphine complexes **4** or **16**, one can mentally strip away all but the *ipso* carbon atoms from the phosphine ligands in Figures 3 and 4. It is clear that in such less congested environments, such as would be experienced with Me₃P ligands (**4**, **16**), the -S-Pt moiety could more readily anchor to any tip or surface. Several platinum alkynyl complexes have been subjected to single molecule measurements, but most of these have featured ligand based thiol groups.²⁴ A well characterized *silver* nanoparticle based assembly that exploits -S-Pt linkages, *trans,trans*-Ag-S-L₂Pt-C≡C-biphenylene-C≡C-PtL₂-S-Ag, has been reported.²³ Here *n*-Bu₃P ligands (L) that are *cis* to the -S-Pt linkage could be successfully employed.

3. Conclusion. This study has provided the first series of longitudinally extended linear polymetallic/sp carbon arrays to be obtained by directed synthesis, as opposed to polymerization or oligomerization. The general methodology can likely be applied to still higher homologs as noted above. The net result is a well defined series of stable, easily handled, functionalizable building blocks that may be of use for molecular devices or new synthetic directions (Scheme 6), and aid in understanding the transition between the molecular and macromolecular limit for polymers that feature metals in the main chain. Strategies for optimizing the anchoring of such complexes via metal-sulfur linkages to noble metal surfaces or STM tips have also been suggested.

Experimental Section

General. Reactions were conducted under dry N₂ atmospheres using standard Schlenk techniques. Workups of platinum complexes were carried out in air. Solvents were treated as follows: THF, Et₂O, and hexane, distilled from Na/benzophenone; acetone, distilled from CaCl₂, CH₂Cl₂, distilled from K₂CO₃; MeOH, distilled from Mg. The following were used as received: *n*-BuLi (1.6 M in hexane, Acros), TMEDA (99%, Janssen), CuCl and CuI (2 × Aldrich, 99.99%, and other sources), HNEt₂ (common commercial sources), *n*-Bu₄N⁺ F⁻ (1.0 M in THF, 5 wt% H₂O, Aldrich), ClSnMe₃ (99%, Acros), ClSiMe₃ (Lancaster), potassium thioacetate (KSAc; Lancaster), Me₃P (1.0 M in toluene, Aldrich), and alumina for chromatography (neutral, Fluka).

NMR spectra were obtained on standard 300 or 400 MHz spectrometers. IR and mass spectra were recorded on ASI React-IR 1000 and Micromass Zabspec instruments, respectively. DSC and TGA data were obtained with a Mettler-Toledo DSC-821 instrument.³⁴ Cyclic voltammograms were recorded as described earlier^{9b} and in Table 7. Microanalyses were conducted on a Carlo Erba EA1110 instrument.

***trans*-Cl(*p*-tol₃P)₂Pt(C≡C)₂SiMe₃ (1).** A round bottom flask was charged with *cis* or *trans*-(*p*-tol₃P)₂PtCl₂ (0.874 g, 1.00 mmol),¹⁶ Me₃Sn(C≡C)₂SiMe₃ (0.285 g, 1.00 mmol), and THF (120 mL), and fitted with a condenser. The solution was refluxed (24 h). The solvent was removed by rotary evaporation and the residue chromatographed on an alumina column (2.5 × 30 cm, 1:3 v/v CH₂Cl₂/hexane). The solvent was removed from the product containing fraction (R_f (TLC) 0.23) by rotary evaporation to give 1 as a pale yellow solid (0.600 g, 0.625 mmol, 63%), dec pt 238 °C (capillary). Calcd for C₄₉H₅₁ClP₂PtSi: C, 61.27; H, 5.35. Found: C, 61.14; H, 5.30.

NMR (δ, CDCl₃): ¹H 7.59-7.54 (m, 12H, *o* to P), 7.17 (d, ³J_{HH} = 7.8 Hz, 12 H, *m* to P), 2.36 (s, 18H, CCH₃), 0.02 (s, 9H, SiCH₃); ¹³C{¹H} 140.5 (s, *p* to P), 134.9 (virtual t, ²J_{CP} = 6.0 Hz,³⁵ *o* to P), 128.7 (virtual t, ³J_{CP} = 5.6 Hz,³⁵ *m* to P), 126.6 (virtual t, ¹J_{CP} = 30.5 Hz,³⁵ *i* to P), 92.7, 87.9 (2t, J_{CP} = 2.3, 3.2 Hz, PtC≡CC), 84.0 (t, ²J_{CP} = 14.8 Hz,

PtC≡), 77.6, (s, ≡CSi), 21.6 (s, CCH₃), 0.4 (s, SiCH₃); ³¹P{¹H} 20.1 (s, ¹J_{Pt} = 2564 Hz).³⁶ IR: Table 1. UV-vis: Table 4. MS³⁷ 960 (9%, [1]⁺), 924 (18%, [1-Cl]⁺), 851 (19%, [1-Cl-SiMe₃]⁺), 803 (100%, [(tol₃P)₂Pt]⁺).

trans-Cl(*p*-tol₃P)₂Pt(C≡C)₂H (2). A round bottom flask was charged with **1** (0.500 g, 0.521 mmol), THF (20 mL), and *n*-Bu₄N⁺ F⁻ (1.0 M in THF/5 wt% H₂O; 0.200 mL, 0.200 mmol). The solution was stirred (0.5 h). Then H₂O (60 mL) was added. The mixture was extracted with CH₂Cl₂ (3 × 80 mL), and the solvent removed by rotary evaporation. The residue was dissolved in THF (2 mL), and MeOH (20 mL) added. The precipitate was collected by filtration and dried by oil pump vacuum to give **2** as a slightly yellow solid (0.443 g, 0.499 mmol, 96%), dec pt 110 °C (capillary). Calcd for C₄₆H₄₃ClP₂Pt: C, 62.20; H, 4.88. Found: C, 62.18; H, 4.86.

NMR (δ, CDCl₃): ¹H 7.58-7.53 (m, 12H, *o* to P), 7.17 (d, ³J_{HH} = 7.8 Hz, 12 H, *m* to P), 2.35 (s, 18H, CH₃), 1.42 (s, 1H, ≡CH); ¹³C{¹H} 140.6 (s, *p* to P), 134.9 (virtual t, ²J_{CP} = 6.3 Hz,³⁵ *o* to P), 128.7 (virtual t, ³J_{CP} = 5.6 Hz,³⁵ *m* to P), 126.5 (virtual t, ¹J_{CP} = 30.3 Hz,³⁵ *i* to P), 86.8 (t, ³J_{CP} = 2.8 Hz, PtC≡C), 80.5 (t, ²J_{CP} = 14.3 Hz, PtC≡), 67.9 (t, ⁴J_{CP} = 2.3 Hz, PtC≡CC), 59.8 (s, ≡CH), 21.6 (s, CCH₃); ³¹P{¹H} 20.2 (s, ¹J_{Pt} = 2560 Hz).³⁶ IR: Table 1. UV-vis: Table 4. MS³⁷ 888 (9%, [2]⁺), 852 (22%, [2-Cl]⁺), 802 (100%, [(tol₃P)₂Pt]⁺).

trans,trans-Cl(*p*-tol₃P)₂Pt(C≡C)₄Pt(*p*-tol₃)₂Cl (3). A three neck flask was charged with **2** (0.300 g, 0.338 mmol) and acetone (23 mL), and fitted with a gas dispersion tube and a condenser. The solution was heated to 30 °C. A Schlenk flask was charged with CuCl (0.230 g, 2.32 mmol) and acetone (23 mL), and TMEDA (0.460 mL, 3.07 mmol) was added with stirring. After 0.5 h, stirring was halted, and a grayish solid separated from a blue supernatant. Then O₂ was bubbled through the three neck flask with stirring. After ca. 5 min, the blue supernatant was added in portions. After 4 h, the solvent was removed by rotary evaporation. The residue was chromatographed on a silica gel column (2.5 × 40 cm, 67:33 v/v CH₂Cl₂/hexane). The solvent was removed

from the product containing fraction (R_f (TLC) 0.48) by rotary evaporation and oil pump vacuum to give **3** as a yellow solid (0.205 g, 0.116 mmol, 68%). The sample slightly darkened at 170 °C, slowly turned black with further heating, and liquefied at 299 °C (capillary). DSC/TGA: Table 3. Calcd for $C_{92}H_{84}Cl_2P_4Pt_2$: C, 62.27; H, 4.77. Found: C, 62.01; H, 5.08.

NMR (δ , $CDCl_3$): 1H 7.56-7.51 (m, 24H, *o* to P), 7.15 (*d*, $^3J_{HH} = 7.8$ Hz, 24H, *m* to P), 2.34 (s, 36H, CH_3); $^{13}C\{^1H\}$ 140.7 (s, *p* to P), 134.8 (virtual t, $^2J_{CP} = 6.1$ Hz,³⁵ *o* to P), 128.4 (virtual t, $^3J_{CP} = 5.4$ Hz,³⁵ *m* to P), 126.4 (virtual t, $^1J_{CP} = 29.8$ Hz,³⁵ *i* to P), 88.5 (s, $PtC\equiv C$), 83.6 (t, $^2J_{CP} = 15.3$ Hz, $PtC\equiv$), 63.4 (s, $PtC\equiv C$), 58.9 (s, $PtC\equiv CC\equiv C$), 21.5 (s, CH_3); $^{31}P\{^1H\}$ 20.1 (s, $^1J_{PPt} = 2553$ Hz).³⁶ IR: Table 1. UV-vis: Table 4. MS³⁷ 1773 ($[3]^+$, 6%), 802 ($[(tol_3P)_2Pt]^+$, 100%), 497 ($[tol_3PPt]^+$, 50%), 405 ($[tol_2PPt]^+$, 92%).

***trans,trans*-Cl(Me₃P)₂Pt(C≡C)₄Pt(PMe₃)₂Cl (4)**. A Schlenk flask was charged with **3** (0.186 g, 0.105 mmol, 1.0 equiv) and CH_2Cl_2 (12 mL). Then Me_3P (1.0 M in toluene; 0.50 mL, 0.50 mmol, 4.8 equiv) was added via syringe. The mixture was stirred until alumina TLC (30/70 v/v CH_2Cl_2 /hexane) showed **3** to be consumed (1 h). The solvents were removed by oil pump vacuum and the residue was filtered through a silica gel column (2 × 5 cm, 85:15 v/v CH_2Cl_2 / MeOH). The solvent was removed from the filtrate by rotary evaporation. The residue was dissolved in CH_2Cl_2 , and hexane was added. The precipitate was collected by filtration and dried by oil pump vacuum to give **4** as a yellow solid (0.078 g, 0.090 mmol, 86%). The sample turned black at 220 °C and remained solid at 330 °C (capillary). Calcd for $C_{20}H_{36}Cl_2P_4Pt_2$: C, 27.88; H, 4.21. Found: C, 27.41; H, 4.20.

NMR (δ , $CDCl_3$): 1H 1.57 (virtual t, $^2J_{HP} = 3.5$ Hz,³⁵ $^3J_{HPt} = 25.6$ Hz,³⁵ 36H, CH_3); $^{13}C\{^1H\}$ 84.7 (s, $PtC\equiv C$), 80.4 (t, $^2J_{CP} = 17.0$ Hz, $PtC\equiv$), 63.5 (s, $PtC\equiv C$), 57.6 (s, $PtC\equiv CC\equiv C$), 13.5 (virtual t, $^1J_{CP} = 19.4$ Hz,³⁵ $^3J_{HPt} = 76.3$ Hz,³⁵ CCH_3); $^{31}P\{^1H\}$ -13.4 (s, $^1J_{PPt} = 2284$ Hz).³⁶ IR: Table 1. MS:³⁷ 861 ($[4]^+$, 100%), 825 ($[4-Cl]^+$, 30%), 749 ($[4-Cl-Me_3P]^+$, 60%).

trans,trans-Cl(*p*-tol₃P)₂Pt(C≡C)₄Pt(P*p*-tol₃)₂(C≡C)₂SiMe₃ (**5**). A round bottom flask was charged with **3** (0.235 g, 0.124 mmol) and CHCl₃ (2.5 mL). A solution of Me₃Sn(C≡C)₂SiMe₃ (0.038 g, 0.13 mmol) in CHCl₃ (2.5 mL) was slowly added by syringe over 4 h with stirring. After another 18 h, the solvent was removed by rotary evaporation. The residue was chromatographed on an alumina column (1 × 40 cm, 2:3 v/v CH₂Cl₂/hexane). The solvent was removed from the product containing fraction (R_f (TLC) 0.60) by rotary evaporation and oil pump vacuum to give **5** as a yellow solid (0.112 g, 0.060 mmol, 46%). The sample slightly darkened at 245 °C, slowly turned black with further heating, and liquefied at 289 °C (capillary). Calcd for C₉₉H₉₃ClP₄Pt₂Si: C, 63.92; H, 5.04. Found: C, 63.48; H, 5.03.

NMR (δ, CDCl₃): ¹H 7.57-7.48 (m, 24H, *o* to P), 7.14 (*d*, ³J_{HH} = 7.7 Hz, 24H, *m* to P), 2.34, 2.33 (2s, 36H, CCH₃), 0.00 (s, 9H, SiCH₃); ¹³C{¹H} 140.7, 140.5 (2s, *p* to P), 134.9, 134.8 (2 virtual t, ²J_{CP} = 4.6, 5.1 Hz,³⁵ *o* to P), 128.7, 128.6 (2 virtual t, ³J_{CP} = 5.6, 5.6 Hz,³⁵ *m* to P), 127.4, 126.5 (2 virtual t, ¹J_{CP} = 30.5, 30.5 Hz,³⁵ *i* to P), 106.1, 105.7 (2t, ¹J_{CP} = 12.8, 14.8 Hz, ≡CPtC≡CC≡CSiMe₃) 83.6 (t, ²J_{CP} = 14.9 Hz, ClPtC≡), 95.9, 95.1, 92.4, 88.6, 68.0, 63.6, 63.3, 59.0, 58.7 (9s, Me₃SiC≡CC≡CPtC≡CC≡CC≡CC), 21.5 (s, CCH₃), 0.3 (s, SiCH₃); ³¹P{¹H} 20.1 (s, ¹J_{PPt} = 2556 Hz),³⁶ 16.8 (s, ¹J_{PPt} = 2523 Hz).³⁶ IR: Table 1. UV-vis: Table 4. MS³⁷ 1857 ([**5**]⁺, 13%), 924 ([(*tol*₃P)₂PtC₄SiMe₃]⁺, 9%) (802 ([(*tol*₃P)₂Pt]⁺, 100%).

trans,trans-Cl(*p*-tol₃P)₂Pt(C≡C)₄Pt(P*p*-tol₃)₂(C≡C)₂H (**6**). A round bottom flask was charged with **5** (0.200 g, 0.108 mmol), CHCl₃ (5 mL), and *n*-Bu₄N⁺ F⁻ (1.0 M in THF/5 wt% H₂O; 0.100 mL, 0.100 mmol). The solution was stirred (24 h). The solvent was removed by oil pump vacuum. The residue was chromatographed on a silica gel column (3 × 30 cm, 1:1 v/v CH₂Cl₂/hexane). The solvent was removed from the product containing fraction by rotary evaporation and oil pump vacuum to give **6** as an orange solid (0.097 g, 0.054 mmol, 50%).

NMR (δ, CDCl₃): ¹H 7.54-7.49 (m, 24H, *o* to P), 7.15 (*d*, ³J_{HH} = 7.3 Hz, 24H, *m*

to P), 2.35, 2.33 (2s, 36H, CH₃), 1.45 (s, 1H, ≡CH); ¹³C{¹H} 140.7, 140.6 (2s, *ρ* to P), 134.9, 134.8 (2 virtual t, ²J_{CP} = 6.1, 6.1 Hz,³⁵ *o* to P), 128.7, 128.6 (2 virtual t, ³J_{CP} = 4.6, 6.1 Hz,³⁵ *m* to P), 127.4, 126.5 (2 virtual t, ¹J_{CP} = 30.5, 29.3 Hz,³⁵ *i* to P), 106.0, 102.6 (2t, ²J_{CP} = 15.2, 15.2 Hz, ≡CPtC≡CC≡CH), 83.7 (t, ²J_{CP} = 13.7 Hz, ClPtC≡), 95.7, 93.9, 88.5, 72.0, 63.6, 63.2, 59.8, 59.0 58.8 (9s, HC≡CC≡CPtC≡CC≡CC≡CC), 21.5 (s, CH₃); ³¹P{¹H} 20.1 (s, ¹J_{PPt} = 2553 Hz),³⁶ 16.7 (s, ¹J_{PPt} = 2534 Hz).³⁶ IR: Table 1. MS³⁷ 1787 ([**6**]⁺, 13%), 1752 ([**6**]⁺-Cl, 5%), 802 ([(tol₃P)₂Pt]⁺, 100%).

trans,trans,trans,trans-Cl(*ρ*-tol₃P)₂Pt(C≡C)₄Pt(P*ρ*-tol₃)₂(C≡C)₄(*ρ*-tol₃P)₂Pt-(C≡C)₄Pt(P*ρ*-tol₃)₂Cl (**7**). **A**. A three neck flask was charged with **6** (0.120 g, 0.0670 mmol) and acetone (20 mL), and fitted with a gas dispersion tube and a condenser. A Schlenk flask was charged with CuCl (0.200 g, 2.02 mmol) and acetone (5 mL), and TMEDA (0.200 mL, 1.33 mmol) was added with stirring. After 0.5 h, stirring was halted, and a grayish solid separated from a blue supernatant. Then O₂ was bubbled through the three neck flask with stirring. After ca. 5 min, the blue supernatant was added in portions. After 6 h, the solvent was removed by rotary evaporation. The residue was chromatographed on a silica gel column (3 × 15 cm, 1:1 v/v CH₂Cl₂/hexane). The solvent was removed from the product containing fraction (R_f (TLC) 0.12) by rotary evaporation and oil pump vacuum to give **7** as an orange solid (0.048 g, 0.013 mmol, 48%). **B**. A three neck flask was charged with **5** (0.200 g, 0.108 mmol) and THF (10 mL), and fitted with a gas dispersion tube and a condenser. Then *n*-Bu₄N⁺ F⁻ (1.0 M in THF/5 wt% H₂O; 0.100 mL, 0.100 mmol) was added with stirring. After 24 h, Me₃SiCl (0.050 mL, 0.40 mmol) was added. After 10 min, acetone (25 mL) was added and the solution was heated to 30 °C. A Schlenk flask was charged with CuCl (0.318 g, 3.21 mmol) and acetone (20 mL), and TMEDA (0.500 mL, 3.33 mmol) was added with stirring. After 0.5 h, stirring was halted, and a greyish solid separated from a blue supernatant. Then O₂ was bubbled through the three necked flask with stirring. After ca. 5 min, the blue supernatant was added in portions. After 4 h, the solvent was removed

by rotary evaporation. The residue was chromatographed on a silica gel column (3 × 25 cm, 1:1 v/v CH₂Cl₂/hexane). The solvent was removed from the product containing fraction (R_f (TLC) 0.11) by rotary evaporation and oil pump vacuum to give **7** as an orange solid (0.151 g, 0.0422 mmol, 79%). The samples slightly darkened at 235 °C and became black at 288 °C (capillary). DSC/TGA: Table 3. Calcd for C₁₉₂H₁₆₈Cl₂P₈Pt₄: C, 64.52; H, 4.74. Found: C, 64.48; H, 5.00.

NMR (δ, CDCl₃): ¹H 7.54-7.45 (m, 48H, *o* to P), 7.14-7.10 (m, 48H, *m* to P), 2.33, 2.32 (2s, 36H, CH₃); ¹³C{¹H} (100 MHz, CDCl₃): 140.7 (s, *p* to P), 134.8, 134.7 (2 virtual t, ²J_{CP} = 6.0, 6.0 Hz,³⁵ *o* to P), 128.6, 128.7 (2 virtual t,³⁵ ³J_{CP} = 5.1, 5.1 Hz, *m* to P), 127.2, 126.5 (2 virtual t,³⁵ ¹J_{CP} = 30.5, 30.5 Hz, *i* to P), 106.1, 105.8 (2t, ²J_{CP} = 16.0, 16.0 Hz, =CPtC=),³⁸ 95.9 (C=CPtC=C), 88.6 (CPtC=C), 83.7 (t, ²J_{CP} = 9.6 Hz, CPtC=), 63.6, 63.4, 63.2, 59.0 (2 × intensity), 58.6 (5s, CPtC=CC=CC=CC=CPtC=CC=C), 21.4 (s, CH₃); ³¹P{¹H} 20.1 (s, ¹J_{Pt} = 2553 Hz),³⁶ 16.7 (s, ¹J_{Pt} = 2520 Hz).³⁶ IR: Table 1. UV-vis: Table 4. MS³⁷ 3574 ([7]⁺, <1%), 802 ([[(tol₃P)₂Pt]⁺, 100%).

trans-H(C≡C)₂Pt(P-*p*-tol₃)₂(C≡C)₂H (8). A. A Schlenk flask was charged with *cis*- or *trans*-(*p*-tol₃P)₂PtCl₂ (0.875 g, 1.00 mmol),¹⁶ CuI (0.060 g, 0.30 mmol), and HNEt₂ (75 mL). The mixture was cooled to -45 °C (CO₂/CH₃CN), and H(C≡C)₂H (1.43 M in THF; 20 mL, 28.6 mmol)³⁹ added with stirring. After 1 h, the cold bath was removed. After another 1.75 h, the solvent was removed by oil pump vacuum. The residue was extracted with toluene (3 × 10 mL). The extracts were filtered through an alumina column (12 cm), which was rinsed with toluene until colorless. The toluene was removed by rotary evaporation. The residue was reprecipitated from CH₂Cl₂/hexane, collected by filtration, and dried by oil pump vacuum to give **8** as a pale yellow solid (0.428 g, 0.475 mmol, 47%). **B.** A Schlenk flask was charged with **9** (0.875 g, 0.836 mmol), THF (20 mL), and *n*-Bu₄N⁺ F⁻ (1.0 M in THF/5 wt% H₂O; 0.200 mL, 0.200 mmol). The solution was stirred (0.5 h). The solvent was removed by oil pump vacuum.

The residue was chromatographed on a silica gel column (3 × 15 cm; 2:3 v/v CH₂Cl₂/hexane). The solvent was removed from the product containing fraction by rotary evaporation and oil pump vacuum to give **8** as a pale yellow solid (0.727 g, 0.806 mmol, 96%). The samples slightly darkened at 170 °C, slowly turned black with further heating, and remained solid at 350 °C (capillary). Calcd for C₅₀H₄₄P₂Pt: C, 66.58; H, 4.92. Found: C, 65.24; H, 4.93.

NMR (δ, CDCl₃): ¹H 7.58-7.53 (m, 12H, *o* to P), 7.17 (d, ³J_{HH} = 7.6 Hz, 12H, *m* to P), 2.36 (s, 18H, *p* to P), 1.46 (s, 2H, ≡CH); ¹³C{¹H} 140.6 (s, *p* to P), 134.8 (virtual t, ²J_{CP} = 6.5 Hz, ³⁵*o* to P), 128.4 (virtual t, ³J_{CP} = 6.1 Hz, ³⁵*m* to P), 127.5 (virtual t, ¹J_{CP} = 30.5 Hz, ³⁵*i* to P), 102.7 (t, ²J_{CP} = 15.3 Hz, PtC≡C), 93.8 (s, PtC≡C), 72.1 (s, C≡CH), 59.7 (s, ≡CH), 21.4 (s, CH₃); ³¹P{¹H} 17.0 (s, ¹J_{PPt} = 2527 Hz).³⁶ IR: Table 1. MS³⁷ 902 ([**8**]⁺, 28%), 852 [(tol₃P)₂PtC₄H]⁺, 46%), 802 [(tol₃P)₂Pt]⁺, 100%).

trans-Me₃Si(C≡C)₂Pt(P-*p*-tol₃)₂(C≡C)₂SiMe₃ (9). A (Scheme 3). A Schlenk flask was charged with *cis*- or *trans*-(*p*-tol₃P)₂PtCl₂ (0.175 g, 0.200 mmol),¹⁶ CuI (0.020 g, 0.11 mmol), HNEt₂ (15 mL), H(C≡C)₂SiMe₃ (0.122 g, 0.998 mmol),⁴⁰ and CH₂Cl₂ (5 mL). The solution was stirred (2 h) and then refluxed (2 h). The solvent was removed by rotary evaporation. The residue was extracted with toluene (3 × 50 mL) The extracts were filtered through a alumina column (7 cm). The solvent was removed by rotary evaporation. The residue was suspended in MeOH (10 mL). The solid was collected by filtration and dried by oil pump vacuum to give **9** as a yellow solid (0.162 g, 0.155 mmol, 78%). **B** (Scheme 5). A Schlenk flask was charged with **3** (0.090 g, 0.051 mmol), CuI (0.005 g, 0.03 mmol), HNEt₂ (10 mL), and H(C≡C)₂SiMe₃ (0.030 g, 0.25 mmol).⁴⁰ The mixture was stirred (23 h). The solvent was removed by oil pump vacuum. The residue was extracted with toluene (3 × 25 mL), and a workup identical to that in A gave **9** as a yellow solid (0.076 g, 0.039 mmol, 77%), dec pt 259 °C (capillary). Calcd for C₅₆H₆₀P₂PtSi₂: C, 64.29; H, 5.78. Found: C, 63.98; H, 5.81.

NMR (δ, CDCl₃): ¹H 7.56-7.51 (m, 12H, *o* to P), 7.16 (d, ³J_{HH} = 7.8 Hz, 12H, *m*

to P), 2.36 (s, 18H, CCH₃), 0.00 (s, 18H, SiCH₃); ¹³C{¹H} 140.3 (s, *p* to P), 134.7 (virtual t, ²J_{CP} = 6.5 Hz,³⁵ *o* to P), 128.5 (virtual t, ³J_{CP} = 5.5 Hz,³⁵ *m* to P), 127.4 (virtual t, ¹J_{CP} = 30.3 Hz,³⁵ *i* to P), 105.9 (t, ²J_{CP} = 14.7 Hz, PtC≡C), 95.2, 92.6 (2s, PtC≡CC), 77.2 (s, ≡CSi), 21.6 (s, CCH₃), 0.4 (s, SiCH₃); ³¹P{¹H} 16.8 (s, ¹J_{PtP} = 2540 Hz).³⁶ IR: Table 1. UV-vis: Table 4. MS³⁷ 1046 ([**9**]⁺, 20%), 924 ([[(tol₃P)₂PtC₄SiMe₃]⁺, 24%), 802 ([[(tol₃P)₂Pt]⁺, 100%).

trans,trans,trans-Cl(*p*-tol₃P)₂Pt(C≡C)₄Pt(P*p*-tol₃)₂(C≡C)₄Pt(P*p*-tol₃)₂Cl (**10**). A three neck flask was charged with **1** (0.500 g, 0.521 mmol), THF (20 mL), and *n*-Bu₄N⁺ F⁻ (1.0 M in THF/5 wt% H₂O; 0.200 mL, 0.200 mmol). The solution was stirred (0.5 h). An IR spectrum showed complete conversion to **2** (2154 cm⁻¹), and Me₃SiCl (0.050 mL, 0.40 mmol) was added. After 10 min, acetone (40 mL) and **8** (0.118 g, 0.131 mmol) were added. A Schlenk flask was charged with CuCl (0.500 g, 5.05 mmol) and acetone (20 mL), and TMEDA (1.00 mL, 6.65 mmol) was added with stirring. After 0.5 h, stirring was halted, and a greyish solid separated from a blue supernatant. Then O₂ was bubbled through the three neck flask with stirring. After ca. 5 min, the blue supernatant was added in portions. After 6 h, the solvent was removed by rotary evaporation. The residue was chromatographed on a silica gel column (3 × 30 cm, 2:1 v/v CH₂Cl₂/hexane). The combined product fractions were taken to dryness and again chromatographed on a silica gel column (3 × 65 cm, 1:1 v/v CH₂Cl₂/hexane). The solvent was removed from the product containing fractions (R_f (THF) 0.14 for **3**, 0.12 for **10**) by rotary evaporation and oil pump vacuum to give **3** as a yellow solid (0.154 g, 0.0868 mmol, 33% based upon **1**) and **10** as an orange solid (0.127 g, 0.0475 mmol, 36% based upon **8**). The sample of **10** slightly darkened at 278 °C, turned black at 288 °C, and liquefied at 308 °C (capillary). DSC/TGA: Table 3. Calcd for C₁₄₂H₁₂₆Cl₂P₆Pt₃: C, 63.77; H, 4.75. Found: C, 63.67; H, 4.88.

NMR (δ, CDCl₃): ¹H 7.55-7.46 (m, 36 H, *o* to P), 7.16-7.12 (m, 36 H, *m* to P), 2.34 (s, 54 H, CH₃); ¹³C{¹H} 140.7 (s, *p* to P), 134.8, 134.7 (2 virtual t, ²J_{CP} = 6.1, 6.1

Hz,³⁵ *o* to P), 128.7 (virtual t, $^3J_{CP} = 5.4$ Hz,³⁵ *m* to P), 127.2, 126.4 (2 virtual t, $^1J_{CP} = 30.5$, 30.5 Hz,³⁵ *i* to P), 105.8 (t, $^2J_{CP} = 15.3$ Hz, $\equiv\text{CPtC}\equiv$), 95.9 (s, $\text{C}\equiv\text{CPTC}\equiv\text{C}$), 88.5 (s, $\text{ClPtC}\equiv\text{C}$), 83.7 (t, $^2J_{CP} = 14.5$ Hz, $\text{ClPtC}\equiv$), 63.6, 63.2, 58.94, 58.86 (4s, $\text{PtC}\equiv\text{CC}\equiv\text{CC}\equiv\text{CC}\equiv\text{CPT}$), 21.4 (s, CH_3); $^{31}\text{P}\{^1\text{H}\}$ 20.1 (s, $^1J_{\text{PPt}} = 2556$ Hz),³⁶ 16.7 (s, $^1J_{\text{PPt}} = 2520$ Hz).³⁶ IR: Table 1. UV-vis: Table 4. MS³⁷ 2675 ($[\text{10}]^+$, 5%), 802 ($[(\text{tol}_3\text{P})_2\text{Pt}]^+$, 100%).

***trans,trans*-Me₃Si(C≡C)₂(*p*-tol₃P)₂Pt(C≡C)₄Pt(*Pp*-tol₃)₂(C≡C)₂SiMe₃ (17).** A round bottom flask was charged with **3** (0.220 g, 0.124 mmol), Me₃Sn(C≡C)₂SiMe₃ (0.075 g, 0.26 mmol), and CHCl₃ (2.5 mL). The solution was stirred (4 h). The solvent was removed by rotary evaporation. The residue was chromatographed on an alumina column (3.5 × 20 cm, 2:3 v/v CH₂Cl₂/hexane). The solvent was removed from the product containing fractions (R_f (TLC) 0.77) by rotary evaporation and oil pump vacuum to give **17** as a yellow solid (0.186 g, 0.0956 mmol, 77%). The sample slightly darkened at 210 °C, slowly turned black with further heating, and remained solid at 330 °C (capillary). DSC: Table 3. Calcd for C₁₀₆H₁₀₂P₄Pt₂Si₂: C, 65.42; H, 5.28. Found: C, 65.39; H, 5.19.

NMR (δ): ^1H (CDCl₃) 7.52-7.47 (m, 24H, *o* to P), 7.13 (d, $^3J_{\text{HH}} = 7.9$ Hz, 24H, *m* to P), 2.34 (s, 36H, CCH₃), 1.45 (s, 18H, SiCH₃); $^{13}\text{C}\{^1\text{H}\}$ (CD₂Cl₂) 141.5 (s, *p* to P), 135.0 (virtual t, $^2J_{CP} = 12.0$ Hz,³⁵ *o* to P), 128.6 (virtual t, $^3J_{CP} = 12.1$ Hz,³⁵ *m* to P), 127.4 (virtual t, $^1J_{CP} = 61.0$ Hz,³⁵ *i* to P), 107.1, 105.9 (2t, $^2J_{CP} = 15.3$, 14.8 Hz, $\equiv\text{CPtC}\equiv$), 95.59, 95.57, 92.6, 77.7, 63.6, 58.8 (6s, $\text{SiC}\equiv\text{CC}\equiv\text{CPTC}\equiv\text{CC}\equiv\text{C}$), 21.6 (s, CCH₃), 0.3 (s, SiCH₃); $^{31}\text{P}\{^1\text{H}\}$ (CDCl₃) 16.6 (s, $^1J_{\text{PPt}} = 2534$ Hz).³⁶ IR: Table 1. UV-vis: Table 4. MS³⁷ 1945 ($[\text{17}]^+$, 8%), 924 ($[(\text{tol}_3\text{P})_2\text{PtC}_4\text{SiMe}_3]^+$, 24%), (803 ($[(\text{tol}_3\text{P})_2\text{Pt}]^+$, 100%).

***trans,trans*-H(C≡C)₂(*p*-tol₃P)₂Pt(C≡C)₄Pt(*Pp*-tol₃)₂(C≡C)₄H (18).** A round bottom flask was charged with **17** (0.285 g, 0.146 mmol) and THF (30 mL). Then *n*-Bu₄N⁺ F⁻ (1.0 M in THF/5 wt% H₂O; 0.400 mL, 0.400 mmol) was added with stirring. After 0.5 h,

the solvent was removed by oil pump vacuum. The residue was chromatographed on a silica gel column (3 × 15 cm, 40:60 v/v CH₂Cl₂/hexane). The solvent was removed from the product containing fractions by rotary evaporation and oil pump vacuum to give **18** as an orange solid (0.252 g, 0.140 mmol, 96%), dec pt 175 °C (capillary). DSC/TGA: Table 3. Calcd for C₁₀₀H₈₆P₄Pt₂: C, 66.66; H, 4.81. Found: C, 67.03; H, 5.38.

NMR (δ, CDCl₃): ¹H 7.54-7.49 (m, 24H, *o* to P), 7.15 (d, ³J_{HH} = 7.8 Hz, 24H, *m* to P), 2.34 (s, 36H, CH₃), 1.45 (s, 2H, ≡CH); ¹³C{¹H} 140.6 (s, *p* to P), 134.7 (virtual t, ²J_{CP} = 12.3 Hz,³⁵ *o* to P), 128.6 (virtual t, ³J_{CP} = 10.7 Hz,³⁵ *m* to P), 127.3 (virtual t, ¹J_{CP} = 61.0 Hz,³⁵ *i* to P), 106.0, 102.6 (2t, ²J_{CP} = 15.3, 15.3 Hz, ≡CPtC≡), 95.7, 93.9, 72.0, 63.4, 59.8, 58.9 (6s, HC≡CC≡CPtC≡CC≡C), 21.4 (s, CH₃); ³¹P{¹H} 16.7 (s, ¹J_{PPt} = 2529 Hz).³⁶ IR: Table 1. UV-vis: Table 4. MS³⁷ 1800 ([**18**]⁺, 13%), 852 ([[(tol₃P)₂PtC₄H]⁺, 15%), (803 [[(tol)₃P)₂Pt]⁺, 100%).

trans-(*p*-tol)(*p*-tol₃P)₂Pt(SAc) (12). A Schlenk flask was charged with *trans*-(*p*-tol)(*p*-tol₃P)₂PtCl (11;^{9b} 0.186 g, 0.200 mmol), KSAc (0.036 g, 0.32 mmol), and CH₂Cl₂ (10 mL). The mixture was stirred (20 h). The solvent was removed by oil pump vacuum. The residue was chromatographed on a silica gel column (2 × 10 cm, CH₂Cl₂). The solvent was removed from the product containing fraction (TLC) by rotary evaporation and oil pump vacuum to give **12** as a white solid (0.145 g, 0.149 mmol, 75%). The sample slightly darkened at 208 °C, slowly turned black with further heating, and liquefied at 238 °C (Capillary). DSC: no endotherm or exotherm below 230 °C. TGA: onset of mass loss, 224 °C. Calcd for C₅₁H₅₂OP₂PtS: C, 63.15; H, 5.40; S, 3.31. Found: C, 62.78; H, 5.64; S, 3.66.

NMR (δ, CDCl₃): ¹H 7.41-7.36 (m, 12H, *o* to P), 7.03 (d, ³J_{HH} = 7.7 Hz, 12H, *m* to P), 6.40 (d, ³J_{HH} = 7.9 Hz, 2H, *o* to Pt), 5.95 (d, ³J_{HH} = 7.7 Hz, 2H, *m* to Pt), 2.30 (s, 18H, PC₆H₄CH₃), 1.88 (s, 3H, PtC₆H₄CH₃), 1.48 (s, 3H, C(O)CH₃); ¹³C{¹H} 204.3 (s, C=O), 141.7 (t, ²J_{CP} = 9.2 Hz, *i* to Pt), 139.3 (s, *p* to P), 137.6 (s, *o* to Pt), 134.6 (virtual t, ²J_{CP} = 6.0 Hz,³⁵ *o* to P), 129.0 (s, *p* to Pt), 128.1 (virtual t, ²J_{CP} = 5.1 Hz,³⁵ *m* to P),

127.9 (s, *m* to Pt), 127.5 (virtual t, $^1J_{CP} = 14.7$ Hz,³⁵ *i* to P), 34.3 (s, C(O)CH₃), 21.4 (s, PC₆H₄CH₃, *p* to P), 20.5 (s, PtC₆H₄CH₃, *p* to Pt); $^{31}\text{P}\{^1\text{H}\}$ 21.1 (s, $^1J_{\text{PPt}} = 3080$ Hz).³⁶ IR (cm⁻¹, powder film) 1613 (m, $\nu_{C=O}$), 946 (m, ν_{C-S}). MS³⁷ 969 ([**12**]⁺, 1%), 894 ([[(tol₃P)₂(tol)Pt]⁺, 45%), 803 ([[(tol₃P)₂Pt]⁺, 100%), 497 ([[tol₃PPT]⁺, 20%), 405 ([[tol₂PPT]⁺, 25%).

***trans,trans*-(AcS)(*p*-tol₃P)₂Pt(C≡C)₄Pt(P*p*-tol₃)₂(SAc) (13)**. A Schlenk flask was charged with **3** (0.177 g, 0.100 mmol), KSAc (0.034 g, 0.30 mmol), and CH₂Cl₂ (10 mL). The mixture was stirred (20 h). The resulting suspension was filtered through an alumina column (2 × 3 cm), which was washed with CH₂Cl₂ (15 mL). The solvent was removed from the combined filtrate by rotary evaporation. Then CH₂Cl₂ (5 mL) was added, followed by hexane to precipitate the product. This procedure was repeated two times. The precipitate was collected by filtration and dried by oil pump vacuum to give **13** as a yellow solid (0.168 g, 0.0906 mmol, 91%). The sample slightly darkened at 258 °C, slowly turned black with further heating, and liquefied at 293 °C (capillary). DSC/TGA: Table 3. Calcd for C₉₆H₉₀O₂P₄Pt₂S₂: C, 62.19; H, 4.89; S, 3.46. Found: C, 62.36; H, 5.14; S, 3.17.

NMR (δ, CDCl₃): ^1H 7.53-7.48 (m, 24H, *o* to P), 7.12 (d, $^3J_{\text{HH}} = 7.8$ Hz, 24H, *m* to P), 2.32 (s, 36H, C₆H₄CH₃), 1.33 (s, 6H, C(O)CH₃); $^{13}\text{C}\{^1\text{H}\}$ 203.0 (s, C=O), 140.3 (s, *p* to P), 134.9 (virtual t, $^2J_{CP} = 6.0$ Hz,³⁵ *o* to P), 128.4 (virtual t, $^3J_{CP} = 5.5$ Hz,³⁵ *m* to P), 127.5 (virtual t, $^1J_{CP} = 30.3$ Hz,³⁵ *i* to P), 95.3 (t, $^2J_{CP} = 15.6$, PtC≡), 93.0 (s, PtC≡C), 63.8, 59.4 (2s, PtC≡CC≡C), 33.3 (s, C(O)CH₃), 21.5 (s, PC₆H₄CH₃, *p* to P); $^{31}\text{P}\{^1\text{H}\}$ 19.4 (s, $^1J_{\text{PPt}} = 2615$ Hz).³⁶ IR: Table 1. UV-vis: Table 4. MS³⁷ 1853 ([**13**]⁺, 5%), 1777 ([[**13**-SAc]⁺, 2%), 1549 ([[**13**-tol₃P]⁺, 10%), 878 ([[(AcS)(tol₃P)₂Pt]⁺, 60%), 803 ([[(tol₃P)₂Pt]⁺, 100%).

***trans,trans,trans*-(AcS)(*p*-tol₃P)₂Pt(C≡C)₄Pt(P*p*-tol₃)₂(C≡C)₄Pt(P*p*-tol₃)₂(SAc) (14)**. Complex **10** (0.170 g, 0.064 mmol), KSAc (0.019 g, 0.17 mmol), and CH₂Cl₂ (12 mL) were combined in a procedure analogous to that for **13**. An identical workup gave

14 as a yellow solid (0.151 g, 0.0548 mmol, 86%). The sample slightly darkened at 208 °C, slowly turned black with further heating, but did not liquefy below 400 °C (capillary). DSC/TGA: Table 3. Calcd for C₁₄₆H₁₃₂O₂P₆Pt₃S₂: C, 63.68; H, 4.83; S, 2.33. Found: C, 64.12; H, 5.37; S, 1.73.

NMR (δ , CDCl₃): ¹H 7.54-7.43 (m, 36H, *o* to P), 7.12, 7.10 (2d, ³J_{HH} = 7.9, 7.8 Hz, 36H, *m* to P), 2.32, 2.31 (2s, 54H, C₆H₄CH₃), 1.33 (s, 6H, C(O)CH₃); ¹³C{¹H} 203.3 (s, C=O), 140.7, 140.4 (2s, *p* to P), 135.0, 134.7 (2 virtual t, ²J_{CP} = 6.2, 6.2 Hz,³⁵ *o* to P), 128.6, 128.5 (2 virtual t, ³J_{CP} = 5.7, 5.7 Hz,³⁵ *m* to P), 127.3, 127.2 (2 virtual t, ¹J_{CP} = 30.5, 30.5 Hz,³⁵ *i* to P), 106.0 (t, ²J_{CP} = 14.5 Hz, ≡CPtC≡), 95.9 (s, C≡CPtC≡C), 95.3 (t, ²J_{CP} = 16.0, SPPtC≡), 93.0 (s, SPPtC≡C), 63.7, 63.6, 59.4, 58.9 (4s, SPPtC≡C≡C≡C≡C≡CPt), 33.2 (s, C(O)CH₃), 21.4 (s, PC₆H₄CH₃, *p* to P); ³¹P{¹H} 19.4 (s, ¹J_{PPt} = 2615 Hz),³⁶ 16.7 (s, ¹J_{PPt} = 2525 Hz).³⁶ IR: Table 1. UV-vis: Table 4. MS³⁷ 2754 ([**42**]⁺, 1%), 2450 ([**14**-Ptol₃]⁺, 1%), 2144 ([**14**-2Ptol₃]⁺, 2%), 878 ([AcS)(tol₃-P)₂Pt]⁺, 42%), 802 ([tol₃P)₂Pt]⁺, 100%).

trans,trans,trans,trans-(AcS)(*p*-tol₃P)₂Pt(C≡C)₄Pt(P*p*-tol₃)₂(C≡C)₄(*p*-tol₃P)₂Pt-(C≡C)₄Pt(P*p*-tol₃)₂(SAC) (**15**). Complex **7** (0.150 g, 0.042 mmol), KSAc (0.014 g, 0.13 mmol), and CH₂Cl₂ (6 mL) were combined in a procedure analogous to that for **13**. An identical workup gave **15** as an orange solid (0.122 g, 0.0334 mmol, 80%). The sample slightly darkened at 158 °C, slowly turned black with further heating, but did not liquefy below 400 °C (capillary). DSC/ TGA: Table 3. Calcd for C₁₉₆H₁₇₄O₂P₈Pt₄S₂: C, 64.43; H, 4.80; S, 1.76. Found: C, 63.47; H, 4.98; S, 1.84.

NMR (δ , CDCl₃): ¹H 7.56-7.45 (m, 48H, *o* to P), 7.14, 7.12 (2d, ³J_{HH} = 7.6, 7.7 Hz, 48H, *m* to P), 2.34, 2.33 (2s, 72H, C₆H₄CH₃), 1.36 (s, 6H, C(O)CH₃); ¹³C{¹H} 203.3 (s, C=O), 140.7, 140.4 (2s, *p* to P), 135.0, 134.6 (2 virtual t, ²J_{CP} = 6.5, 6.5 Hz,³⁵ *o* to P), 128.6, 128.5 (2 virtual t, ³J_{CP} = 5.5, 5.5 Hz,³⁵ *m* to P), 127.21, 127.19 (2 virtual t, ¹J_{CP} = 30.5, 30.5 Hz,³⁵ *i* to P), 106.0 (t, ²J_{CP} = 17.1 Hz, ≡CPtC≡ these two carbon are not same but have same chemical shifts), 95.9 (s, C≡CPtC≡C), 95.3 (t, ²J_{CP} = 15.3,

SPtC≡), 92.9 (s, SPtC≡C), 67.9, 63.7, 63.5, 63.4, 59.3, 58.9 (2 × intensity) (6s, SPtC≡CC≡CC≡CC≡CPtC≡CC≡C), 33.1 (s, C(O)CH₃), 21.4 (s, PC₆H₄CH₃, *p* to P); ³¹P{¹H} 19.4 (s, ¹J_{PPt} = 2614 Hz),³⁶ 16.7 (s, ¹J_{PPt} = 2518 Hz).³⁶ IR: Table 1. UV-vis: Table 4. MS³⁷ 3651 ([15]⁺, < 1%), 3043 ([15–2tol₃P]⁺, 1%), 878 ([AcS)(tol₃P)₂Pt]⁺, 28%), 802 ([tol₃P)₂Pt]⁺, 100%).

***trans,trans*-(AcS)(Me₃P)₂Pt(C≡C)₄Pt(PMe₃)₂(SAc) (16).** A Schlenk flask was charged with **4** (0.084 g, 0.098 mmol, 1.0 equiv), CH₂Cl₂ (12 mL), and KSAc (0.033 g, 0.292 mmol). The mixture was stirred until silica TLC (98:2 v/v CH₂Cl₂/MeOH) showed no **4** or monosubstituted intermediate (18 h). The solvent was removed by oil pump vacuum and CH₂Cl₂ added. The sample was filtered through a silica gel column (2 × 5 cm) that was washed with CH₂Cl₂/MeOH (98:2 v/v). The solvent was removed from the eluate by rotary evaporation. The residue was dissolved in CH₂Cl₂, and hexane was added. The precipitate was collected by filtration and dried by oil pump vacuum to give **16** as a yellow solid (0.070 g, 0.074 mmol, 76%). The sample darkened at 255 °C and remained solid at 330 °C (capillary). Calcd for C₂₄H₄₂O₂P₄Pt₂S₂: C, 30.64; H, 4.50; S, 6.82. Found: C, 30.39; H, 4.92; S, 6.81.

NMR (δ, CDCl₃): ¹H 2.32 (s, 6H, C(O)CH₃), 1.59 (virtual t, ²J_{HP} = 3.3 Hz,³⁵ ³J_{HPt} = 27.8 Hz,³⁵ 36H, PCH₃); ¹³C{¹H} 205.0 (s, C=O), 94.4 (t, ²J_{CP} = 16.0, PtC≡), 88.7 (s, PtC≡C), 63.7 (s, PtC≡CC), 58.3 (s, PtC≡CC≡C), 34.8 (s, C(O)CH₃), 14.3 (virtual t, ¹J_{CP} = 19.7 Hz,³⁵ ²J_{CPt} = 78.0 Hz,³⁵ PCH₃); ³¹P{¹H} –17.1 (s, ¹J_{PPt} = 2318 Hz).³⁶ IR: Table 1. MS:³⁷ 940 ([16]⁺, 100%), 865 ([16–SAc]⁺, 60%), 519 ([AcS(Me₃P)₂PtC₈+H]⁺, 10%).

Me₃Sn(C≡C)₂SiMe₃.¹⁵ A Schlenk flask was charged with H(C≡C)₂SiMe₃ (0.788 g, 6.45 mmol)⁴⁰ and Et₂O (30 mL). The solution was cooled to –78 °C, and *n*-BuLi (2.5 M in hexane; 2.6 mL, 6.5 mmol) was added with stirring. After 1 h, the cold bath was removed, and Me₃SnCl (1.285 g, 6.449 mmol) was added. After 3 h, the reaction cold saturated aqueous NH₄Cl was added (50 mL). The aqueous phase was extracted with hexane (3 × 30 mL), and the combined organic phases were dried (MgSO₄). The

solvents were removed by rotary evaporation. The residue was dried by oil pump vacuum to give $\text{Me}_3\text{Sn}(\text{C}\equiv\text{C})_2\text{SiMe}_3$ as a white solid (1.618 g, 5.676 mmol, 88%).

NMR (δ , CDCl_3): ^1H 0.29 (s, $^2J_{\text{HSn}} = 58 \text{ Hz}$,⁴¹ 9H, SnCH_3), 0.15 (s, 9H, SiCH_3); ^{13}C { ^1H } 91.3, 88.1, 87.8, 83.0 (s, $\text{C}\equiv\text{CC}\equiv\text{C}$), -0.5 (s, SiCH_3), -7.8 (s, $^1J_{\text{CSn}} = 397 \text{ Hz}$,⁴¹ SnCH_3). IR (cm^{-1} , powder film): 2192/2054 (w/m, $\nu_{\text{C}\equiv\text{C}}$).

Crystallography. A. Acetone vapor was allowed to diffuse into a CH_2Cl_2 solution of **3** at room temperature. After one week, the yellow prisms were taken to a Nonius KappaCCD area detector for data collection as outlined in Table 5. Cell parameters were obtained from 10 frames using a 10° scan and refined with 9740 reflections. Lorentz, polarization, and absorption corrections⁴² were applied. The space group was determined from systematic absences and subsequent least squares refinement. The structure was solved by direct methods. The parameters were refined with all data by full-matrix-least-squares on F^2 using SHELXL.⁴³ Non-hydrogen atoms were refined with anisotropic thermal parameters. The hydrogen atoms were fixed in idealized positions using a riding model. For every molecule of **3**, two disordered acetone molecules were also present. The structure exhibited an inversion center at the midpoint of C4-C4'. Scattering factors were taken from literature.⁴⁴ **B.** Acetone vapor was allowed to diffuse into a CH_2Cl_2 solution of **17** at room temperature. After two weeks, the yellow prisms were analyzed as described for **3** (cell parameters from 10 frames using a 10° scan; refined with 15 reflections). The structure was solved and refined as with **3**, and exhibited an inversion center at the midpoint of C5-C5'. **C.** A CH_2Cl_2 solution of **12** was layered with MeOH and kept at room temperature. After two days, the white prisms were analyzed as described for **3** (cell parameters from 10 frames using a 10° scan; refined with 9464 reflections). The structure was solved and refined as with **3**.

ORCID ●

John A. Gladysz: 0000-0002-7012-4872;

Hashem Amini: 0000-0002-9921-9816

v ACKNOWLEDGEMENT

We thank the Deutsche Forschungsgemeinschaft (DFG, SFB 583) and the US National Science Foundation (CHE-1566601) for support and Dr. Tobias Fiedler for assistance with some of the graphics.

References

(1) (a) Paul, F.; Lapinte, C. in *Unusual Structures and Physical Properties in Organometallic Chemistry*, Gielen, M.; Willem, R.; Wrackmeyer, B. Eds; Wiley: New York, 2002, pp. 220-291. (b) Szafert, S.; Gladysz, J. A. *Chem. Rev.* **2003**, *103*, 4175-4205 and *Chem. Rev.* **2006**, *106*, PR1-PR33. (c) Bruce, M. I.; Low, P. J. *Adv. Organomet. Chem.* **2004**, *50*, 179-444. (d) Gückel, S.; Gluyas, J. B. G.; El-Tarhuni, S.; Sobolev, A. N.; Whiteley, M. W.; Halet, J.-F.; Lapinte, C.; Kaupp, M.; Low, P. J. *Organometallics* **2018**, *37*, 1432-1445, and earlier papers cited therein. (e) Pigulski, B.; Gulia, N.; Szafert, S. *Eur. J. Org. Chem.* **2019**, *2019*, 1420-1445.

(2) (a) Tanaka, Y.; Kiguchi, M.; Akita, M. *Chem. Eur. J.* **2017**, *23*, 4741-4749. (b) Tanaka, Y.; Kato, Y.; Tada, T.; Fujii, S.; Kiguchi, M.; Akita, M. *J. Am. Chem. Soc.* **2018**, *140*, 10080-10084.

(3) (a) ALQaisi, S. M.; Galat, K. J.; Chai, M.; Ray, D. G., III; Rinaldi, P. L.; Tessier, C. A.; Youngs, W. J. *J. Am. Chem. Soc.* **1998**, *120*, 12149-12150. (b) Bruce, M. I.; Costuas, K.; Halet, J.-F.; Hall, B. C.; Low, P. J.; Nicholson, B. K.; Skelton, B. W.; White, A. H. *J. Chem. Soc., Dalton Trans.* **2002**, *31*, 383-398. (c) Bruce, M. I.; Zaitseva, N. N.; Nicholson, B. K.; Skelton, B. W.; White, A. H. *J. Organomet. Chem.* **2008**, *693*, 2887-2897. (d) Kohn, D. R.; Gawel, P.; Xiong, Y.; Christensen, K. E.; Anderson, H. L. *J. Org. Chem.* **2018**, *83*, 2077-2086.

(4) (a) Takahashi, S.; Kariya, M.; Yatake, T.; Sonogashira, K.; Hagihara, N. *Macromolecules* **1978**, *11*, 1063-1066 and preliminary communications cited therein. (b) Sonogashira, K.; Kataoka, S.; Takahashi, S.; Hagihara, N. *J. Organomet. Chem.* **1978**, *160*, 319-327. (c) Sonogashira, K.; Ohga, K.; Takahashi, S.; Hagihara, N. *J. Organomet. Chem.* **1980**, *188*, 237-243. (d) Review: Hagihara, N.; Sonogashira, K.; Takahashi, S. *Adv. Polym. Sci.* **1981**, *41*, 149-179.

(5) (a) Fujikura, Y.; Sonogashira, K.; Hagihara, N. *Chem. Lett.* **1975**, 1067-1070. (b) Takahashi, S.; Murata, E.; Sonogashira, K.; Hagihara, N. *J. Polym. Sci., Polym.*

Chem. **1980**, *18*, 661-669.

(6) (a) Lewis, J.; Khan, M. S.; Kakkar, A. K.; Johnson, B. F. G.; Marder, T. B.; Fyfe, H. B.; Wittmann, F.; Friend, R. H.; Dray, A. E. *J. Organomet. Chem.* **1992**, *425*, 165-176. (b) Markwell, R. D.; Butler, I. S.; Kakkar, A. K.; Khan, M. S.; Al-Zakwani, Z. H.; Lewis, J. *Organometallics* **1996**, *15*, 2331-2337.

(7) See the following studies and references therein: (a) Khan, M. S.; Al-Mandhary, M. R. A.; Al-Suti, M. K.; Corcoran, T. C.; Al-Mahrooqi, Y.; Atfield, J. P.; Feeder, N.; David, W. I. F.; Shankland, K.; Friend, R. H.; Köhler, A.; Marseglia, E. A.; Todesco, E.; Tang, C. C.; Raithby, P. R.; Collings, J. C.; Roscoe, K. P.; Batsanov, A. S.; Stimson, L. M.; Marder, T. B. *New. J. Chem.* **2003**, *27*, 140-149. (b) La Groia, A.; Ricci, A.; Bassetti, M.; Masi, D.; Bianchini, C.; Lo Sterzo, C. *J. Organomet. Chem.* **2003**, *683*, 406-420. (c) Khan, M. S.; Al-Mandhary, M. R. A.; Al-Suti, M. K.; Al-Battashi, F. R.; Al-Saadi, S.; Ahrens, B.; Bjernmose, J. K.; Mahon, M. F.; Raithby, P. R.; Younus, M.; Chawdhury, N.; Köhler, A.; Marseglia, E.; Tedesco, E.; Feeder, N.; Teat, S. J. *Dalton Trans.* **2004**, *33*, 2377-2385. (d) Wong, W.-Y.; Ho, C.-L. *Coord. Chem. Rev.* **2006**, *250*, 2627-2690.

(8) (a) Brady, M.; Weng, W.; Zhou, Y.; Seyler, J. W.; Amoroso, A. J.; Arif, A. M.; Böhme, M.; Frenking, G.; Gladysz, J. A. *J. Am. Chem. Soc.* **1997**, *119*, 775-788. (b) Dembinski, R.; Bartik, T.; Bartik, B.; Jaeger, M.; Gladysz, J. A. *J. Am. Chem. Soc.* **2000**, *122*, 810-822. (c) Meyer, W. E.; Amoroso, A. J.; Horn, C. R.; Jaeger, M.; Gladysz, J. A. *Organometallics* **2001**, *20*, 1115-1127. (d) Horn, C. R.; Gladysz, J. A. *Eur. J. Inorg. Chem.* **2003**, *9*, 2211-2218.

(9) (a) Mohr, W.; Stahl, J.; Hampel, F.; Gladysz, J. A. *Chem. Eur. J.* **2003**, *9*, 3324-3340. (b) Zheng, Q.; Bohling, J. C.; Peters, T. B.; Frisch, A. C.; Hampel, F.; Gladysz, J. A. *Chem. Eur. J.* **2006**, *12*, 6486-6505. (c) Stahl, J.; Mohr, W.; de Quadras, L.; Peters, T. B.; Bohling, J. C.; Martín-Alvarez, J. M.; Owen, G. R.; Hampel, F.; Gladysz, J. A. *J. Am. Chem. Soc.* **2007**, *129*, 8282-8295. (d) de Quadras, L.; Bauer, E.

B.; Mohr, W.; Bohling, J. C.; Peters, T. B.; Martín-Alvarez, J. M.; Hampel, F.; Gladysz, J. A. *J. Am. Chem. Soc.* **2007**, *129*, 8296-8309. (e) de Quadras, L.; Bauer, E. B.; Stahl, J.; Zhuravlev, F.; Hampel, F.; Gladysz, J. A. *New. J. Chem.* **2007**, *31*, 1594-1604. (f) Owen, G. R.; Stahl, J.; Hampel, F.; Gladysz, J. A. *Chem. Eur. J.* **2008**, *14*, 73-87. (g) Owen, G. R.; Gauthier, S.; Weisbach, N.; Hampel, F.; Bhuvanesh, N.; Gladysz, J. A. *Dalton Trans.* **2010**, *39*, 5260-5271. (h) Baranová, Z.; Amini, H.; Bhuvanesh, N.; Gladysz, J. A. *Organometallics* **2014**, *33*, 6746-6749. (i) Zhang, T.; Bhuvanesh, N.; Gladysz, J. A. *Eur. J. Inorg. Chem.* **2017**, *2017*, 1017-1025.

(10) Chalifoux, W. A.; Tykwinski, R. R. *Nature Chem.* **2010**, *2*, 967-971

(11) (a) Tour, J. M. *Acc. Chem. Res.* **2000**, *33*, 791-804. (b) Xiang, D.; Wang, X.; Jia, C.; Lee, T.; Guo, X. *Chem. Rev.* **2016**, *116*, 4318-4440.

(12) Zheng, Q.; Hampel, F.; Gladysz, J. A. *Organometallics* **2004**, *23*, 5896-5899.

(13) Ballmann, S.; Hieringer, W.; Secker, D.; Zheng, Q.; Gladysz, J. A.; Görling, A.; Weber, H. B. *ChemPhysChem* **2010**, *11*, 2256-2260.

(14) Li, Y.; Winkel, R. W.; Weisbach, N.; Gladysz, J. A.; Schanze, K. S. *J. Phys. Chem. A* **2014**, *118*, 10333-10339.

(15) Bunz, U. H. F.; Enkelmann, V. *Organometallics* **1994**, *13*, 3823-3833 (see footnote 14 therein).

(16) The yields given are for reactions with the *cis* isomer, which is the major product obtained from K_2PtCl_4 and *p*-tol₃P: (a) Alt, H. G.; Baumgärtner, R.; Brune, H. A. *Chem. Ber.* **1986**, *119*, 1694-1703. (b) Matern, E.; Pikies, J.; Fritz, G. *Z. Anorg. Allg. Chem.* **2000**, *626*, 2136-2142.

(17) When *cis*-(*p*-tol₃P)₂PtCl₂ is employed in Scheme 1, the reflux period is essential to isomerize the *cis* product to the *trans* product. This is unnecessary for the reactions in Scheme 3.

(18) Cardin, C. J.; Cardin, D. J.; Lappert, M. F. *J. Chem. Soc., Dalton Trans.* **1977**, 767-779.

(19) Grim, S. O.; Keiter, R. L.; McFarlane, W. *Inorg. Chem.* **1967**, *6*, 1133-1137.

(20) Hay, A. S. *J. Org. Chem.* **1962**, *27*, 3320-3321.

(21) Sonogashira, K.; Yatake, T.; Tohda, Y.; Takahashi, S.; Hagihara, N. *J. Chem. Soc. Chem. Commun.* **1977**, 291-292.

(22) The *n*-Bu₃P analog of **8**, and the Ph₃P analog of **9**, have been previously characterized: (a) Sonogashira, K.; Fujikura, Y.; Yatake, T.; Toyoshima, N.; Takahashi, S.; Hagihara, N. *J. Organomet. Chem.* **1978**, *145*, 101-108. (b) Peters, T. B.; Zheng, Q.; Stahl, J.; Bohling, J. C.; Arif, A. M.; Hampel, F.; Gladysz, J. A. *J. Organomet. Chem.* **2002**, *641*, 53-61.

(23) For a relevant study employing silver nanoparticles, see Battocchio, C.; Fratoddi, I.; Fontana, L.; Bodo, E.; Porcaro, F.; Meneghini, C.; Pis, I.; Nappini, S.; Mobilio, S.; Russo, M. V.; Polzonetti, G. *Phys.Chem.Chem.Phys.* **2014**, *16*, 11719-11728.

(24) (a) Mayor, M.; von Hänisch, C.; Weber, H. B.; Reichert, J.; Beckmann, D. *Angew. Chem. Int. Ed.* **2002**, *41*, 1183-1186; *Angew. Chem.* **2002**, *114*, 1228-1231. (b) Schull, T. L.; Kushmerick, J. G.; Patterson, C. H.; George, C.; Moore, M. H.; Pollack, S. K.; Shashidhar, R. *J. Am. Chem. Soc.* **2003**, *125*, 3202-3203. (c) Schwarz, F.; Kastlunger, G.; Lissel, F.; Egler-Lucas, C.; Semenov, S. N.; Venkatesan, K.; Berke, H.; Stadler, R.; Lörtscher, E. *Nature Nanotechnology* **2016**, *11*, 170-176.

(25) Neo, Y. C.; Vittal, J. J.; Hor, A. *J. Organomet. Chem.* **2001**, *637-639*, 757-761.

(26) (a) Baddour, F. G.; Hyre, A. S.; Guillet, J. L.; Pascual, D.; Lopez-de-Luzuriaga, J. M.; Alam, T. M.; Bacon, J. W.; Doerrer, L. H. *Inorg. Chem.* **2017**, *56*, 452-469 (see Figure 4). (b) Yoshida, T.; Cosquer, G. Izuogu, D. C.; Ohtsu, H.; Kawano, M.; Lan, Y.; Wernsdorfer, W.; Nojiri, H.; Breedlove, B. K.; Yamashita, M. *Chem. Eur. J.* **2017**, *23*, 4551-4556 (see Figure 1c therein).

(27) Hexaruthenium complexes with RuRu(C≡C)₂RuRu(C≡C)₂RuRu segments

have also been described: (a) Ying, J.-W.; Liu, I. P.-C.; Xi, B.; Song, Y.; Campana, C.; Zuo, J.-L.; Ren, T. *Angew. Chem. Int. Ed.* **2010**, *49*, 954-957; *Angew. Chem.* **2010**, *122*, 966-969. (b) Ying, J.-W.; Cao, Z.; Campana, C.; Song, Y.; Zuo, J.-L.; Tyler, S. F.; Ren, T. *Polyhedron*, **2015**, *86*, 76-80.

(28) Weng, W.; Bartik, T.; Brady, M.; Bartik, B.; Ramsden, J. A.; Arif, A. M.; Gladysz, J. A. *J. Am. Chem. Soc.* **1995**, *117*, 11922-11931.

(29) Some preliminary studies have been carried out. The mixture of **10** and **3** obtained in Scheme 3 was treated with excess $\text{Me}_3\text{Sn}(\text{C}\equiv\text{C})_2\text{SiMe}_3$. Column chromatography afforded pure *trans,trans,trans*- $\text{Me}_3\text{Si}(\text{C}\equiv\text{C})_2(\textit{p}\text{-tol}_3\text{P})_2\text{Pt}(\text{C}\equiv\text{C})_4\text{Pt}(\textit{P}\textit{p}\text{-tol}_3)_2(\text{C}\equiv\text{C})_4\text{Pt}(\textit{P}\textit{p}\text{-tol}_3)_2(\text{C}\equiv\text{C})_2\text{SiMe}_3$, which was completely characterized. Weisbach, N. doctoral dissertation, Universität Erlangen-Nürnberg, 2011, pp 39-42.

(30) (a) Lissel, F.; Fox, T.; Blacque, O.; Polit, W.; Winter, R. F.; Venkatesan, K.; Berke, H. *J. Am. Chem. Soc.* **2013**, *135*, 4051-4060. (b) Schwarz, F.; Kastlunger, G.; Lissel, F.; Riel, H.; Venkatesan, K.; Berke, H.; Stadler, R.; Lörtscher, E. *Nano Lett.* **2014**, *14*, 5932-5940. (c) see also Semenov, S. N.; Taghipourian, S. F.; Blacque, O.; Fox, T.; Venkatesan, K.; Berke, H. *J. Am. Chem. Soc.* **2010**, *132*, 7584-7585.

(31) Analogous substitutions have been carried out with bis(alkynyl) monoplatinum complexes *trans*- $(\text{Ar}_3\text{P})_2\text{Pt}(\text{C}\equiv\text{CR})_2$: Sadowy, A. L.; Ferguson, M. J.; McDonald, R.; Tykwinski, R. R. *Organometallics* **2008**, *27*, 6321-6325.

(32) Ehnbohm, A.; Hall, M.; Gladysz, J. A. *Org. Lett.* **2019**, *20*, 753-757.

(33) Tour, J. M.; Jones II, L. R.; Pearson, D. L.; Lamba, J. J. S.; Burgin, T. P.; Whitesides, G. M.; Allara, D. L.; Parikh, A. N.; Atre, S. V. *J. Am. Chem. Soc.* **1995**, *117*, 9529-9534.

(34) Data were treated as recommended by Cammenga, H. K.; Epple, M. *Angew. Chem., Int. Ed. Engl.* **1995**, *34*, 1171-1187; *Angew. Chem.* **1995**, *107*, 1284-1301. The T_g values best represent the temperature of the phase transition.

(35) For virtual triplets (Hersh, W. H. *J. Chem. Educ.* **1997**, *74*, 1485-1488), the

$^xJ_{CP}$ or $^xJ_{HP}$ values represent *apparent* couplings between adjacent peaks that take place through a minimum of x bonds.

(36) This coupling represents a satellite (d; $^{195}\text{Pt} = 33.8\%$), and is not reflected in the peak multiplicity given.

(37) FAB, 3-NBA, m/z (relative intensity, %); the most intense peak of the isotope envelope is given.

(38) The triplets at 106.1 and 105.8 ppm are poorly resolved, and the uncertainties in the chemical shifts and coupling constants are somewhat greater than for the other signals.

(39) Verkruijsse, H. D.; Brandsma, L. *Synth. Commun.* **1991**, *21*, 657-659. The $\text{H}(\text{C}=\text{C})_2\text{H}$ concentration is calculated from the mass increase of the THF solution. This compound is reported to be explosive.

(40) Bartik, B.; Dembinski, R.; Bartik, T.; Arif, A. M.; Gladysz, J. A. *New J. Chem.* **1997** *21*, 739-750.

(41) This coupling represents a satellite (d; $^{119}\text{Sn} = 8.58\%$), and is not reflected in the peak multiplicity given.

(42) (a) "Collect" data collection software, Nonius B.V., 1998. (b) "Scalepack" data processing software: Otwinowski, Z.; Minor, W. in *Methods in Enzymology* **1997**, *276*, 307-326 (Macromolecular Crystallography, Part A), 307.

(43) Sheldrick, G. M. *Acta. Cryst. C* **2015**, *71*, 3-8.

(44) Cromer, D. T.; Waber, J. T. In *International Tables for X-ray Crystallography*, Ibers, J. A., Hamilton, W. C., Eds.; Kynoch: Birmingham, England, 1974.

Table 1. $^{31}\text{P}\{^1\text{H}\}$ NMR (CDCl_3) and IR (powder film) data.

Complex	IR $\nu_{\text{C}\equiv\text{C}}$ (cm^{-1})	$^{31}\text{P}\{^1\text{H}\}$ NMR (δ , ppm) [$^1J_{\text{PPt}}$, Hz]
1	2194/2124 w/m	20.1 [2564]
2	2154 s ^a	20.2 [2560]
8	2146 s	17.0 [2527]
9	2189/2127 m/s	16.8 [2540]
3	2139/2008 m/w	20.1 [2553]
4	2150/2007 m/w	-13.4 [2284]
5	2185/2135/2043/2003 w/s/w/m	16.8 [2523], 20.1 [2556]
6	2147/2008 s/w ^a	16.7 [2534], 20.1 [2553]
17	2196/2135/2034/1999 w/s/w/w	16.6 [2534]
18	2135/1996 s/m	16.7 [2529]
10	2142/2003 s/m	16.7 [2520], 20.1 [2556]
7	2138/1999 s/m	16.7 [2520], 20.1 [2553]
13	2150/2011 m/w ^b	19.4 [2615]
14	2144/1999 m/w ^b	16.7 [2525], 19.4 [2615]
15	2142/2003 m/w ^b	16.7 [2518], 19.4 [2614]
16	2142/1999 s/m ^b	-17.1 [2318]

^a $\nu_{\text{C-H}}$ (w-m) 3289 (2), 3267 (6). ^b $\nu_{\text{C=O}}/\nu_{\text{C-S}}$ (m/m) 1617/946 (13), 1613/946 (14), 1625/946 (15), 1621/942 (16).

Table 2. $^{13}\text{C}\{^1\text{H}\}$ NMR data (δ , ppm; CDCl_3).

Comple x	XPtC \equiv [$^2J_{\text{CP}}$, Hz] ^a	XPtC \equiv C	\equiv CPtC \equiv [$^2J_{\text{CP}}$, Hz] ^a	C \equiv CPtC \equiv C	other C \equiv C
3 ^b	83.6 [15.3]	88.5	-	-	63.4, 58.9
4 ^b	80.4 [17.0]	84.7	-	-	63.5, 57.6
5 ^b	83.6 [14.9]	-	106.1 [12.8], 105.7 [14.8]	-	95.9, 95.1, 92.4, 88.6, 68.0, 63.6, 63.3, 59.0, 58.7
6 ^b	83.7 [13.7]	-	106.0 [15.2], 102.6 [15.2]	-	95.7, 93.9, 88.5, 72.0, 63.6, 63.2, 59.8, 59.0, 58.8
17 ^c	-	-	107.1 [15.3], 105.9 [14.8]	-	95.59, 95.57, 92.6, 77.7, 63.6, 58.8
18	-	-	106.0 [15.3], 102.6 [15.3]	-	95.7, 93.9, 72.0, 63.4, 59.8, 58.9
10 ^b	83.7 [14.5]	88.5	105.8 [15.3]	95.9	63.6, 63.2, 58.94, 58.86
7 ^b	83.7 [15.3]	88.6	106.1 [16.0], 105.8 [16.0]	95.9	63.6, 63.4, 63.2, 59.0 (double intensity), 58.6
13 ^d	95.3 [15.6]	93.0	-	-	63.8, 59.4

14^d	95.3 [16.0]	93.0	106.0 [14.5]	95.9	63.7, 63.6, 59.4, 58.9
15^d	95.3 [15.3]	92.9	106.0 [17.1]	95.9	67.9, 63.7, 63.5, 63.4, 59.3, 58.9 (double intensity)
16^d	94.4[16.0]	88.7	-	-	63.7, 58.3

^a All signals with *J* values are triplets. ^b X = Cl. ^c data recorded in CD₂Cl₂. ^d X = S.

Table 3. Thermal stability data (°C).

complex	mass loss (onset)	DSC	decomposition (onset) capillary thermolysis ^b
	TGA	T/T _d /T _d /T _d /T _d ^a	
3	285	174/187/200/213/223 ^c	170 ^d
10	294	193/198/203/213/225 ^c	288 ^d
7	284	184/193/195/203/212 ^c	235 ^d
17	-	163/171/174/175/178 ^c 268/276/279 ^c	210 ^d
18	179	169/175/179 ^e	175 ^d
13	289	290 ^f	293 ^g
14	231	240 ^f	208 ^d
15	246	183/192/205/215/222 ^c	158 ^d

^a See reference 34 for definitions. ^b Sealed; conventional melting point apparatus. ^c Exotherm. ^d Decomposition without melting. ^e Endotherm. ^f No endotherm or exotherm below this temperature. ^g Decomposition with melting; some darkening above 258 °C.

Table 4. UV/Visible data (CH₂Cl₂, 1.25 × 10⁻⁵ M in complex).

Complex	absorption (nm) [ε (M ⁻¹ cm ⁻¹)]
1	257 [39700], 294 [7920]
2	257 [43000], 299 [8320]
9	314 [10600], 334 [30200]
3	267 [119000], 324 [80300], 360 [21500], 388 [10800], 421 [6160]
5	266 [111000], 311 [66900], 344 [104000], 391 [21400], 424 [11400]
17	300 [79000], 354 [113000], 393 [31000], 426 [16200]
18	300 [70800], 350 [105000], 392 [24100], 425 [13000]
10	312 [97400], 353 [153000], 367 [139000], 397 [59800], 432 [36400]
7	308 [128000], 356 [200000], 371 [236000], 400 [112000], 436 [64600]
13	337 [87000], 388 [10900], 420 [5800]
14	303 [105000], 354 [153000], 366 [146000], 398 [63200], 432 [37400]
15	304 [158000], 356 [248000], 368 [263000], 399 [114000], 435 [67000]

Table 5. Summary of Crystallographic Data.

Complex	3 ·(acetone) ₂	17	12
empirical formula	C ₉₈ H ₉₆ Cl ₂ O ₂ P ₄ Pt ₂	C ₁₀₆ H ₁₀₂ P ₄ Pt ₂ Si ₂	C ₅₁ H ₅₂ OP ₂ PtS
formula weight	1890.70	1946.11	970.01
temperature [K]	173(2)	173(2)	173(2)
Diffractometer	Nonius Kappa CCD	Nonius MACH3	Nonius Kappa CCD
wavelength [Å]	0.71073	0.71073	0.71073
crystal system	monoclinic	triclinic	triclinic
space group	P2 ₁ /c	P-1	P-1
unit cell dimensions:			
<i>a</i> [Å]	11.20880(10)	11.607(8)	10.9509(2)
<i>b</i> [Å]	37.2486(3)	14.949(6)	12.22430(10)
<i>c</i> [Å]	11.55030(10)	15.867(11)	17.8210(3)
α [°]	90	93.57(4)	70.7936(9)
β [°]	113.2910(10)	108.77(5)	84.6362(8)
γ [°]	90	96.43(5)	75.8053(10)
<i>V</i> [Å ³]	4429.41(7)	2576(3)	2183.86(6)
<i>Z</i>	2	1	2
ρ _{calc} [Mg/m ⁻³]	1.418	1.254	1.475
μ [mm ⁻¹]	3.334	2.839	3.370
<i>F</i> (000)	1900	982	980
crystal size [mm ³]	0.30 × 0.30 × 0.15	0.30 × 0.30 × 0.10	0.20 × 0.20 × 0.15
θ limit [°]	1.09 to 27.48	3.65 to 26.35	1.92 to 27.51
index range (<i>h</i> , <i>k</i> , <i>l</i>)	-14, 14; -48, 48; -14, 14	-14, 13; -18, 18; 0, 19	-14, 14; -15, 15; -23, 23
reflections collected	18516	10788	18891
independent reflections	10055	10398	10006
<i>R</i> (int)	0.0284	0.0940	0.0185
completeness to θ	99.0	98.7	99.6
max. and min. transmission	0.6346 and 0.4345	0.7644 and 0.4830	0.6318 and 0.5521
data/restraints/parameters	10055/0/506	10398/0/502	10006/0/505
goodness-of-fit on <i>F</i> ²	1.040	0.977	1.070
<i>R</i> indices (final) [<i>I</i> > 2σ(<i>I</i>)]			
<i>R</i> ₁	0.0292	0.0743	0.0237
<i>wR</i> ₁	0.0695	0.1566	0.0597
<i>R</i> indices (all data)			
<i>R</i> ₂	0.0492	0.1358	0.0276
<i>wR</i> ₂	0.0915	0.1858	0.0612
largest diff. peak and hole [eÅ ⁻³]	0.78 and -0.98	2.08 and -1.46	0.93 and -1.40

Table 6. Key interatomic distances (Å) and bond angles (°) for diplatinum complexes.

Complex	3 ·(acetone) ₂	17
Pt-C ₁	1.935(4)	1.972(11)
C ₁ ≡C ₂	1.208(5)	1.204(16)
C ₂ -C ₃	1.367(6)	1.350(18)
C ₃ ≡C ₄ or C ₃ ≡C ₅	1.201(6)	1.208(19)
C ₄ -C _{4'} or C ₅ -C _{5'}	1.375(9)	1.39(3)
Pt-Cl	2.3481(10)	-
Pt-P ₁	2.3144(10)	2.306(3)
Pt-P ₂	2.3216(10)	2.314(3)
Pt-C ₁₁	-	1.970(10)
C ₁₁ ≡C ₁₂	-	1.223(13)
C ₁₂ -C ₁₃	-	1.379(14)
C ₁₃ ≡C ₁₄	-	1.199(15)
C ₁₄ -Si ₁	-	1.809(12)
Pt-Pt'	12.7498(3)	12.833
Cl-Cl' or Si-Si'	17.422	27.629
C ₁ -Pt-Cl or C ₁ -Pt-C ₁₁	178.13(11)	176.7(6)
P ₁ -Pt-P ₂	177.11(3)	174.41(13)
C ₁ -Pt-P ₁	86.27(11)	92.7(3)
C ₁ -Pt-P ₂	91.34(11)	88.4(3)
P ₁ -Pt-Cl or P ₁ -Pt-C ₁₁	95.56(3)	89.2(3)
P ₂ -Pt-Cl or P ₂ -Pt-C ₁₁	86.85(4)	89.4(3)
Pt ₁ -C ₁ -C ₂	178.7(4)	176.0(12)
C ₁ -C ₂ -C ₃	174.1(5)	179(3)
C ₂ -C ₃ -C ₄ or C ₂ -C ₃ -C ₅	175.3(5)	177(2)
C ₃ -C ₄ -C _{4'} or C ₃ -C ₅ -C _{5'}	178.3(7)	171(6)
Pt-C ₁₁ -C ₁₂	-	173.0(10)
C ₁₁ -C ₁₂ -C ₁₃	-	172.4(11)
C ₁₂ -C ₁₃ -C ₁₄	-	177.5(13)
C ₁₃ -C ₁₄ -Si	-	178.3(12)

Table 7. Cyclic voltammetry data.^a

Complex	E _{p,a} [V]	E _{p,c} [V]	E° [V]	ΔE [mV]	i _c /i _a
3	1.17	1.06	1.12	103	0.94
5	1.16	1.08	1.12	80	0.82
17	1.18	1.10	1.14	80	0.79
10	1.15	1.06	1.10	94	0.53
7	1.21	1.07	1.14	143	0.52
12	1.12	-	-	-	≤0.05
13	1.18	-	-	-	0
14	1.12	-	-	-	0
15	1.22	-	-	-	0

^a Conditions: 3-11 × 10⁻⁴ M in substrate and 0.10 M in *n*-Bu₄N⁺ BF₄⁻ in CH₂Cl₂ at 22.5 ± 1 °C; Pt working and counter electrodes, potential vs. Ag wire pseudoreference; scan

rate 100 mV/s, calibrated vs. added ferrocene = 0.46 V.

TABLE OF CONTENTS GRAPHIC

The title complexes are accessed from platinum chloride and $Z(\text{C}\equiv\text{C})_2\text{SiMe}_3$ ($Z = \text{Me}_3\text{Sn}, \text{H}$) building blocks via oxidative homocouplings and cross couplings.

